Computers & Industrial Engineering 175 (2023) 108900

Contents lists available at ScienceDirect

Computers & Industrial Engineering

journal homepage: www.elsevier.com/locate/caie

Effect of measurement uncertainty on combined quality control charts

Tahir Munir [a], Xuelong Hu [b], Osmo Kauppila [c,d,*], Bjarne Bergquist [d]

[a] Department of Anaesthesiology, The Aga Khan University Karachi, Pakistan
[b] School of Management, Nanjing University of Posts and Telecommunications, Nanjing, China
[c] Industrial Engineering and Management, University of Oulu, Finland
[d] Quality Technology and Logistics, Luleå University of Technology, Luleå, Sweden

ARTICLE INFO

Keywords:
Measurement Uncertainty
Statistical Process Control
Combined Control Chart
Multiple Measurements
Reliability Monitoring
Monte Carlo Simulation

ABSTRACT

The accuracy of the measurement system is vital for reliable process monitoring using statistical process control charts. The applied chart's effectiveness depends on the measurement system's performance. Measurement uncertainty can lead to incorrect decisions like unnecessary stops or failure to intervene. In this paper, we investigated the effect of measurement errors on the performance of four well-established combined charts for monitoring the mean of normally distributed processes: Shewhart-CUSUM, Shewhart-Crosier's CUSUM, Shewhart-EWMA and Shewhart-GWMA charts. To deal with measurement errors we considered the additive measurement error model. Detailed run length profiles of these charts are studied in terms of average run length (ARL), extra quadratic loss, relative ARL, and performance comparison index through Monte Carlo simulations under different sizes of measurement errors. It was found that measurement errors significantly reduce the power of the combined charts. Thus, multiple measurements scheme is incorporated as a remedy to this effect. The Shewhart-Crosier's CUSUM performed best of four charts, while the Shewhart-EWMA chart did worst. To demonstrate the effect of measurement uncertainty and highlight implications further, a simulated dataset with a shift in the process mean is considered.

1. Introduction

There are many tools in the Statistical Process Control (SPC) toolkit, which are extensively used in modern industries to monitor and control both manufacturing and service processes. SPC is a powerful collection of problem-solving tools for achieving process stability and improving capability by reducing variability (cf. Montgomery, 2012). The univariate control chart is one of the essential SPC tools to detect process changes affecting the monitored entity, so called shifts, and it was developed by Shewhart (1924).

Generally, we may classify charts into memory-less and memory-type. Shewhart-type charts are memory-less, and their main strength is to detect large shifts quickly. They are, however, less sensitive to small and moderate shifts in the process parameters (location and dispersion). As an improvement of the memory-less monitoring chart, the cumulative sum (CUSUM) chart (Page, 1954) and the exponentially weighted moving average (EWMA) chart (Roberts, 1959) improved the detection power of small shifts. These memory-type charts use both past and current information, making them more sensitive to small and moderate shifts in the process parameters, at the expense of being slower to detect large shifts. Later on, improvements have been proposed to these two charts by Crosier (1986), such as Crosier's CUSUM (CCUSUM) and Sheu & Lin (2003) suggested the generally weighted moving average (GWMA) charts.

To combine the strengths and mitigate the weaknesses of memory-less and memory-type charts, Lucas (1982) proposed a combined chart known as Shewhart-CUSUM, enabling one chart to monitor both small-to-moderate and large size shifts. He discovered that the Shewhart-CUSUM chart outperformed the standard CUSUM and Shewhart (when shift $< 3\sigma$) charts in terms of average run-length (ARL). The CUSUM chart performed as well for small shifts (when shift $< 1.5\sigma$), but less efficiently for moderate-to-large shifts. When the shift size greater than 3σ, the Shewhart chart was more efficient than the Shewhart-CUSUM chart. He advised that the Shewhart-CUSUM chart is not robust to outliers while being simple to implement. Similarly to Lucas (1982), Lucas & Saccucci (1990) proposed the Shewhart-EWMA chart to improve detection power of the EWMA chart. It was discovered that the Shewhart-EWMA was more sensitive than EWMA by itself. They also

* Corresponding author at: Industrial Engineering and Management, University of Oulu, Finland.
E-mail addresses: tmunir@stat.qau.edu.pk, tahirmunir677@yahoo.com (T. Munir), hxl0419@njupt.edu.cn (X. Hu), Osmo.Kauppila@oulu.fi (O. Kauppila), Bjarne.Bergquist@ltu.se (B. Bergquist).

https://doi.org/10.1016/j.cie.2022.108900
Received 3 July 2022; Received in revised form 1 December 2022; Accepted 8 December 2022
Available online 13 December 2022

suggested using Shewhart limits larger than in a standard Shewhart chart to avoid a large reduction in the IC ARL. Furthermore, they advised against using the Shewhart-EWMA chart whenever the process produces occasional outliers.

More recently, Sheu & Lin (2003) proposed the Shewhart-GWMA chart for enhancing detection ability of the GWMA chart against large shifts. They recommended that this chart may be preferable if detecting small shifts in the process mean is more important than avoiding spending time or cost on false alarms identification. Later, Rehman et al. (2022) proposed the Shewhart-CCUSUM chart, following Lucas (1982), and revealed that this chart was slightly more effective for small shifts ($< 0.50\sigma$) than the Shewhart-CUSUM chart, while other held the same properties. However, in most practical process settings, predicting the exact size of shifts from the target value is difficult. Combined charts are considered powerful SPC tools for monitoring both small-to-moderate and moderate-to-large process shifts, while simple to implement by attaching the additional Shewhart limits to the memory-type charts without designing complex charting structures.

Generally, in SPC, the standard assumption is that observations from the underlying process are recorded through a perfect measurement system. However, in a practical SPC application, this assumption is violated as numerous factors influence the characteristic(s) of interest when measuring observations, including environmental (e.g., temperature and light), human (e.g., improper operation and error collection), and even the measurement system itself. These factors are inevitable in measurement processes, and they introduce errors into true observations (cf., Maleki et al., 2017; Bennett, 1954). Measurement error is the difference between a characteristic's recorded and true value. On a production line, for instance, it is impossible to measure the exact volume of liquid contained in bottles; measurement errors usually occur during the generation and measurement of peak areas during mass-spectrometry analyses in analytical laboratories; likewise, analogue blood pressure machines used in medical settings might not always give accurate readings, (Riaz, 2014). This variation results in increased observed process variability and may result in adversarial effects through incorrect deductions and decisions. Therefore, an accurate measuring system with an observed mean close to the true value and high precision is important (International Organization for Standardization, 1994). Regarding charts, their statistical performance will also degrade with increasing measurement variation for a given process variation (Linna, & Woodall, 2001). Imprecise measurements increase the rate of false alarms in IC situations, and significantly reduce the charts' abilities to detect out-of-control (OC) situations.

Bennett (1954) was the pioneer to investigate the effect of measurement errors on the $\overline{X}$ chart using an additive model $Y = X + \varepsilon$. This was followed by Abraham (1977) in the 1970s, and interest has increased particularly in the 2000s as computational scenarios have become more accessible and new techniques have been proposed. Early on, Kanazuka (1986) examined the chart's power in the presence of measurement error for the process average and variance. The effect of measurement error on the performance of $\overline{X}$ and S^2 charts was investigated by Linna and Woodall (2001) using a linear covariate model. The loss of power in detecting parameter shifts in the underlying process variable is one of the effects of measurement error, and they found that multiple measurements for each item in a subgroup could be desirable, (Linna, & Woodall, 2001).

In very recent research, Ayooub et al. (2020) proposed a coefficient of variations chart under measurement errors, while Nguyen et al. (2021) explored the impact of measurement error on EWMA chart performance for the ratio of two normally distributed variables. Thanwane et al. (2021) studied the performance of the homogenously weighted moving average *X*monitoring chart under the measurement errors, and Umar et al. (2022) examined how measurement errors affected the effectiveness of the triple sampling (TS) $\overline{X}$chart. The performance of the GWMA chart was investigated in Li et al. (2022) in the presence of measurement errors for monitoring two parameter exponential distribution. Raiz et al. (2021) studied the impact of measurement error on the joint monitoring of process mean and coefficient of variation. For monitoring the mean of a multivariate normally distributed processes in in Phase II, Yousefi et al. (2022) explored the effects of measurement system incapability on the sensitivity of multivariate homogeneously weighted moving average chart. In order to track the shifts in the process coefficient of variation parameter of the multivariate process under measurement error for Phase II, Hemmati et al. (2022) proposed a run sum chart. Their studies used the linear covariate error model for constant and linearly increasing variance.

However, to the best of our knowledge, no previous research studies have investigated the effect of measurement errors on combined Shewhart-CUSUM, Shewhart-CCUSUM, Shewhart-EWMA, and Shewhart-GWMA charts, despite them being an appealing option for SPC practitioners as they depend on commonly known and available methods. Therefore, it is essentially important to improve the performance of combined charts in the presence of measurement errors. This paper aims to complete this research gap by focusing on decision risks caused by measurement uncertainty on combined charts for the mean of normally distributed processes. Furthermore, we study a multiple measurement strategy to remedy the variation caused by measurement errors.

The structure of the rest of this paper is as follows: Section 2 provides a brief review of four combined quality charts without measurement error. Section 3 introduces the same four quality charts, including measurement uncertainty. The results come from Monte Carlo simulations, and Section 4 presents measurement uncertainty analysis on different charts. Section 5 provides an illustrative example based on a simulated real-life situation, and concluding remarks are in Section 6.

2. A review of the four combined quality control charts

This section gives a brief overview of some existing combined charts when the interest lies in rapidly detecting both large and small shifts in the process mean of a normally distributed process.

Let $\{Y_t; t \geq 1\}$ be the underlying quality characteristic, distributed as $N(\mu, \sigma^2)$ at time $t \geq 1$. A random sample of size $n : (Y_{t,1}, Y_{t,2}, \cdots, Y_{t,n})$ is repeatedly drawn from the process, and the value of the sample mean $\overline{Y}_t = \frac{Y_{t,1}+Y_{t,2}+\cdots+Y_{t,n}}{n}$ at the time t is computed to monitor the changes in the process mean μ. In correspondence to the $\{Y_t\}$, $\{Y_t; t \geq 1\}$, $\overline{Y}_t$ is a sequence of independently and identically normally distributed random variables with mean $\mu_{\overline{Y}} = \mu$ and standard deviation $\sigma_{\overline{Y}} = \frac{\sigma}{\sqrt{n}}$.

We consider the process to be IC when the process mean $\mu = \mu_0$ and has shifted to an OC state $\mu = \mu_1 = \mu_0 + \Delta \times \frac{\sigma}{\sqrt{n}}$. Here $\Delta = \frac{(\mu_1-\mu_0)\sqrt{n}}{\sigma}$ is the standardized shift leading to the new OC mean.

2.1. The Shewhart-CUSUM chart

Lucas (1982) integrated the Shewhart chart with the CUSUM chart into the Shewhart-CUSUM chart. The Shewhart-CUSUM chart works similarly to the classical CUSUM chart to monitor the process mean μ using the sequence $\{\overline{Y}_t\}$. The chart works with the two upward and downward CUSUM statistics, say A_t^+ and A_t^-, respectively, along with the Shewhart chart, given by

$$\left.\begin{aligned} A_t^+ &= max[0, A_{t-1}^+ + (\overline{Y}_t - \mu_0) - K] \\ A_t^- &= \max[0, A_{t-1}^- - (\overline{Y}_t - \mu_0) - K] \end{aligned}\right\}, \tag{1}$$

where $K = k\sigma/\sqrt{n}$ is the slack value of the Shewhart-CUSUM chart. Here, a common choice of k is half of the magnitude of the shift δ of the process mean that one wishes to detect, i.e., $k = \delta/2$ for the CUSUM parametric setting.

The upper control limit (UCL) and the lower control limit (LCL) of the Shewhart chart based on $\overline{Y}_t$, are given by

$$\mathrm{UCL} = \mu_0 + \mathrm{L}_1\frac{\sigma}{\sqrt{n}} \quad and \quad \mathrm{LCL} = \mu_0\text{-}\mathrm{L}_1\frac{\sigma}{\sqrt{n}} \tag{2}$$

where L_1 is an arbitrarily chosen constant selected to get the desired IC ARL. The two-sided Shewhart-CUSUM chart declares the OC process if $\overline{Y}_t$ exceeds the control limits given in Eq. (2) in either direction, or either A_t^+ or A_t^- exceeds the predetermined decision value $H = h\sigma/\sqrt{n}$. The values of h are also selected to get the desire IC ARL of the Shewhart-CUSUM chart.

2.2. The Shewhart-Crosier CUSUM chart

Crosier (1986) proposed a more sensitive CUSUM chart over the classical one by Page (1954), namely the CCUSUM chart. Based on this chart, Rehman et al. (2022) proposed the new two-sided Shewhart-CCUSUM chart for efficiently monitoring the process mean. This chart is based on the following statistics:

$$\left.\begin{array}{c} B_t = 0, if C_t \le K \\ B_t = (\overline{Y}_t - \mu_0 + B_{t-1})(1 - K/C_t), if C_t > K \end{array}\right\}, \tag{3}$$

where $C_t = |\overline{Y}_t - \mu_0 + B_{t-1}|$ and $B_0 = 0$. Here, the reference parameter K and the control limits H, LCL and UCL of the Shewhart-CCUSUM chart are similar to those of the Shewhart-CUSUM chart in Section 2.1. The two-sided Shewhart-CCUSUM chart triggers an OC signal whenever $B_t > H$ or $B_t < -H$ and/or $\overline{Y}_t < LCL$ or $\overline{Y}_t > UCL$. Unlike the Shewhart-CUSUM statistics (A_t^+, A_t^-), the CUSUM statistic B_t is first updated with $\overline{Y}_t$, and then it is shrunk towards zero, which makes the chart more powerful for detecting small shifts.

2.3. The Shewhart-EWMA chart

To make the EWMA chart more sensitive to large shifts in the process target value, Lucas and Saccucci (1990) considered a combined Shewhart-EWMA chart. By using the sequence of $\{\overline{Y}_t\}$, let D_t be the ordinary EWMA statistic, defined as

$$D_t = \lambda\overline{Y}_t + (1-\lambda)D_{t-1}, \tag{4}$$

where λ is the smoothing constant ranging between zero and one. The user usually chooses λ below 0.5 to make the chart more sensitive to small shifts. The mean and standard deviation of the statistic D_t are respectively:

$$\mathrm{E}(D_t) = \mu \tag{5}$$

and

$$Std(D_t) = \frac{\sigma}{\sqrt{n}}\sqrt{\frac{\lambda}{(2-\lambda)}[1-(1-\lambda)^{2t}]}$$

Here, the term $[1-(1-\lambda)^{2t}]$ approaches unity as t increases. The asymptotic variance of the EWMA statistic D_t is given by:

$$Std(D_t) = \frac{\sigma}{\sqrt{n}}\sqrt{\frac{\lambda}{(2-\lambda)}} \tag{6}$$

When the process is IC, the control limits of the EWMA chart based on the asymptotic variance of D_t are given by

$$\left.\begin{array}{l} UCL = \mu_0 + L_2\frac{\sigma}{\sqrt{n}}\sqrt{\frac{\lambda}{2-\lambda}} \\ LCL = \mu_0 - L_2\frac{\sigma}{\sqrt{n}}\sqrt{\frac{\lambda}{2-\lambda}} \end{array}\right\}. \tag{7}$$

The Shewhart-EWMA chart triggers an OC signal when either D_t falls outside the EWMA control limits or $\overline{Y}_t$ falls outside the Shewhart control limits in Eq. (2). Here, L_2 and L_1 are the design parameters of the Shewhart-EWMA chart, respectively, and their values depend on the choices of λ and the desired IC ARL.

2.4. The Shewhart-GWMA chart

Sheu and Lin (2003) proposed the GWMA chart as a more sensitive alternative to the EWMA. Furthermore, they suggested the combined Shewhart-GWMA chart as an improvement on the Shewhart-EWMA chart. Let α and $q \in [0,1]$ be the adjustment and design parameters of the Shewhart-GWMA chart. Then, based on $\{\overline{Y}_t\}$, let $\{E_t\}$ be a GWMA sequence, given by,

$$E_t = (q^{0^\alpha} - q^{1^\alpha})\overline{Y}_t + (q^{1^\alpha} - q^{2^\alpha})\overline{Y}_{t-1} + (q^{(t-1)^\alpha} - q^{t^\alpha})\overline{Y}_1 + q^{t^\alpha}\mu_Y \tag{8}$$

where $t = 1, 2, \cdots$ Since E_t is a linear combination of $\overline{Y}_t$, E_t is also a normal random variable with the mean μ and the variance $Q_t\sigma^2$, where $Q_t = (q^{0^\alpha} - q^{1^\alpha})^2 + (q^{1^\alpha} - q^{1^\alpha})^2 + \cdots + (q^{(t-1)^\alpha} - q^{t^\alpha})^2$, i.e., $E_t \sim N(\mu, Q_t\sigma^2/n)$. The UCL and LCL of the GWMA chart in the combined Shewhart-GWMA chart at time t are,

$$\left.\begin{array}{c} \mathrm{UCL}_t = \mu_0 + \mathrm{L}_3\frac{\sigma}{\sqrt{n}}\sqrt{Q_t} \\ \mathrm{CL}_t = \mu_0 \\ \mathrm{LCL}_t = \mu_0 - \mathrm{L}_3\frac{\sigma}{\sqrt{n}}\sqrt{Q_t} \end{array}\right\}, \tag{9}$$

where the value of L_3 is selected in conjunction with the value of L_1 such that the resulting IC ARL of the Shewhart-GWMA chart reaches the desired level, and CL_t is the central line representing the expected mean of the chart. The chart gives an OC signal whenever either $E_t > UCL_t$ or $E_t < LCL$, or $\overline{Y}_t$ falls beyond the limits in Eq. (2), respectively. The selections of α and q depend on the chart's RL performance. For detecting small size shifts, the GWMA chart outperforms the EWMA chart when $q > 0.5$ and $0.5 \le \alpha \le 0.90$. We note that when $\alpha = 1$ and $q = 1-\lambda$, the Shewhart-GWMA chart reduces to the Shewhart-EWMA chart, where $\lambda \in (0,1]$ is the smoothing constant of the EWMA statistic. Moreover, the GWMA chart in the Shewhart-GWMA chart reduces to the classical Shewhart chart when $\alpha = 1$ and $q = 0$.

3. Four combined quality control charts with a measurement uncertainty

Next, we present how we treat the four control charts presented in Section 3, including measurement uncertainty. Let the consecutive observations of the quality characteristic Y, at the time t = 1,2,…, be $\{Y_{t,1}, Y_{t,2}, \cdots, Y_{t,n}\}$. As stated in Section 3, we assume that the $Y_{t,j}$'s are independent normal random variables with the nominal mean $\mu_0 + \Delta\sigma$ and the standard-deviation σ, i.e., $Y_{i,j}$ $N(\mu_0 + \Delta\sigma, \sigma)$. As suggested by Linna and Woodall (2001), we also assume that the quality characteristic $Y_{t,j}$ is not directly observable, but can only be assessed from the results $\{X_{t,j,1}, X_{t,j,2}, \cdots, X_{t,j,m}\}$ of a set of $m \ge 1$ measurement operations, with each $X_{i,j,k}$ being equal to (so-called linearly covariate error model). In other words,

$$X_{t,j,k} = A + BY_{t,j} + \varepsilon_{t,j,k} \tag{10}$$

where A and B are two known constants while $\varepsilon_{t,j,k}$ is a normal random error term due to the measurement inaccuracy, i.e. ε $N(0, \sigma_M)$, which is also independent of $Y_{t,j}$. The measurement error variance $\sigma_M{}^2$ can be a

constant independent of the nominal mean μ_0 or, as mentioned in Linna and Woodall (2001), it can sometimes linearly depend on $\mu = \mu_0 + \Delta\sigma$ (say ${\sigma_M}^2 = C + D\mu$, where C and D are two constants). The measurement error may also include a constant misrepresentation, e.g., due to poor calibration. For simplicity, we only focus on the former case, i.e. the measurement error variance is a constant and is independent of the nominal mean, and the mean of the error is zero. We can apply similar methods to the linearly increasing measurement error case.

Since we assume $X_{t,j,k}$ comes from an imperfect measurement system, then it is standard practice to take multiple measurements per item (i.e., using an m-measurements strategy with $m \geq 1$) as a remedial approach to reduce the measurement error effect, as suggested by Linna and Woodall (2001). Averaging several measurements per item reduces the error variance compared to measuring only once. However, practitioners must choose the appropriate value of m to balance the extra costs and time associated with the multiple measurements and an acceptable level of measurement errors.

At time $t = 1, 2, \cdots$, as $j = 1, 2, \cdots, n$ and $k = 1, 2, \cdots, m$, we have $m \times n$ observations $X_{t,j,k}$ and the sample mean $\overline{X}_t$ equals to

$$\overline{X}_t = \frac{1}{mn}\sum_{j=1}^{n}\sum_{k=1}^{m} X_{t,j,k} = A + \frac{1}{n}\left(B\sum_{j=1}^{n} Y_{t,j} + \frac{1}{m}\sum_{j=1}^{n}\sum_{k=1}^{m}\varepsilon_{t,j,k}\right). \tag{11}$$

It can easily be proven that the expectation $E(\overline{X}_t)$ and the variance $V(\overline{X}_t)$ of X_t are equal to

$$E(\overline{X}_t) = A + B(\mu_0 + \Delta\sigma), \tag{12}$$

and

$$V(\overline{X}_t) = \left(B^2\sigma^2 + \frac{\sigma_M^2}{m}\right), \tag{13}$$

or equivalently

$$V(\overline{X}_t) = \frac{B^2\sigma^2}{nC^2_{(n,m,\gamma)}} \tag{14}$$

where

$$C^2 = \frac{m}{m + (\sigma_M/\sigma_0)^2} = \frac{m}{m + \gamma^2}$$

and $\gamma = \frac{\sigma_M}{\sigma_0}(\gamma > 0)$ denotes the ratio of the measurement system variability to the process variability.

3.1. The measurement uncertainty-based Shewhart-CUSUM chart

By using the sequence of $\{\overline{X}_t\}$, the two-sided Shewhart-CUSUM chart can be constructed for monitoring the process mean under the presence of measurement uncertainty. The Shewhart-CUSUM chart uses the plotting-statistics, say (D_t^+, D_t^- and $\overline{X}_t$) at the time t,

$$\left.\begin{aligned} D_t^+ &= max[0, +(\overline{X}_t - \mu_X) - K + D_{t-1}^+] \\ D_t^- &= max[0, -(\overline{X}_t - \mu_X) - K + D_{t-1}^-] \end{aligned}\right\}. \tag{15}$$

The control limits for the Shewhart chart are

$$\frac{\mathrm{LCL}}{\mathrm{UCL}} = \mu_X \mp \mathrm{L}_1\frac{\sigma_X}{\sqrt{n}}, \tag{16}$$

where the initial values of D_0^+ and D_0^- are set to be 0. $K = k\sigma_X/\sqrt{n}\,(> 0)$ and $H = h\sigma_X/\sqrt{n}(> 0)$ are the reference parameter and control limit of the CUSUM chart. The values of k, h and L_1 are selected to maintain the IC ARL at a specific level. The OC signal initiated by the two-sided Shewhart-CUSUM chart whenever (D_t^+ and/or $D_t^- > H$) and ($\overline{X}_t >$ UCL and/or $\overline{X}_t < LCL$).

3.2. The measurement uncertainty-based Shewhart-CCUSUM chart

The two-sided Shewhart-CCUSUM chart considers the following plotting-statistics for monitoring the irregular changes in the process mean parameter when there is measurement uncertainty, based on the sequence.$\{\overline{X}_t\}$

$$\left.\begin{aligned} E_t &= 0, && \text{if } F_t \leq K \\ E_t &= (\overline{X}_t - \mu_X + E_{t-1})(1 - K/F_t), && \text{if } F_t > K \end{aligned}\right\}, \tag{17}$$

where $E_0 = 0$ and $F_t = |\overline{X}_t - \mu_X + E_{t-1}|$. The reference sensitive parameter $K = k\sigma_X/\sqrt{n}$ and $H = h\sigma_X/\sqrt{n}$ is the decision interval of the Shewhart-CCUSUM chart. The values of K, H and L_1 are chosen to reach a desired IC ARL. Whenever $E_t > H$ or $E_t < -H$ and/or $\overline{X}_t < LCL$ or$\overline{X}_t >$ UCL, the two-sided Shewhart-CCUSUM chart triggers an OC signal.

3.3. The measurement uncertainty-based Shewhart-EWMA chart

In the presence of measurement uncertainty, it is possible to design the Shewhart-EWMA chart using the sequence $\{\overline{X}_t\}$, for monitoring shifts in the process location parameter μ_X. This chart considers the following plotting-statistics, say $\{G_t\}$, defined as:

$$G_t = \lambda\overline{X}_t + (1 - \lambda)G_{t-1}. \tag{18}$$

Like the λ value of the Shewhart-EWMA chart, the λ for the uncertainty-based EWMA chart is usually set to a value less than 0.5 to improve small shift sensitivity. $G_0 = \mu_X$ represents the starting value of the monitored response property.

The mean and asymptotic variance of the statistic G_t are respectively:

$$\mathrm{E}(G_t) = \mu_X \tag{19}$$

and

$$V(G_t) = \frac{\sigma_X}{\sqrt{n}}\sqrt{\frac{\lambda}{2 - \lambda}}. \tag{20}$$

In the Shewhart-EWMA chart, UCL and LCL of the EWMA chart based on the asymptotic variance of G_t are given by:

$$\left.\begin{aligned} UCL &= \mu_X + \mathrm{L}_2\frac{\sigma_X}{\sqrt{n}}\sqrt{\frac{\lambda}{2 - \lambda}} \\ CL &= \mu_X, \\ LCL &= \mu_X - \mathrm{L}_2\frac{\sigma_X}{\sqrt{n}}\sqrt{\frac{\lambda}{2 - \lambda}} \end{aligned}\right\}. \tag{21}$$

The design parameters, L_1 in Eq. (16) and L_2 of the Shewhart-EWMA chart and their values are selected according to the choices of λ and the desired IC ARL. The process is considered OC when either G_t falls outside the EWMA control limits or $\overline{X}_t$ falls outside the Shewhart control limits in Eq. (16), triggering remedial action.

3.4. The measurement uncertainty-based Shewhart-GWMA chart

The Shewhart-GWMA chart can also be constructed for monitoring infrequent process mean changes in the presence of measurement uncertainty. Based on $\{\overline{X}_t\}$, this chart considers the following statistics:

$$H_t = \left(q^{0^\alpha} - q^{1^\alpha}\right)\overline{X}_t + \left(q^{1^\alpha} - q^{2^\alpha}\right)\overline{X}_{t-1} + \left(q^{(t-1)^\alpha} - q^{t^\alpha}\right)\overline{X}_1 + q^{t^\alpha}\mu_X, \tag{22}$$

where H_t is a linear combination of $\overline{X}_t$ and it is a normal random variable with mean μ_X and variance $Q_t{\sigma_X}^2$ i.e., $H_t \sim N(\mu_X, Q_t{\sigma_X}^2/n)$ where $Q_t = (q^{0^\alpha} - q^{1^\alpha})^2 + (q^{1^\alpha} - q^{1^\alpha})^2 + \cdots + (q^{(t-1)^\alpha} - q^{t^\alpha})^2$, where, in turn, $q \in [0, 1)$ is the design/smoothing parameter and $\alpha > 0$ is the adjustment parameter determined by the practitioner. The UCL, CL and

LCL of the GWMA chart in the Shewhart-GWMA chart, at the time t, are:

$$\left.\begin{aligned} \mathrm{UCL}_t &= \mu_X + \mathrm{L}_3\frac{\sigma_X}{\sqrt{n}}\sqrt{Q_t} \\ \mathrm{CL}_t &= \mu_X \\ \mathrm{LCL}_t &= \mu_X - \mathrm{L}_3\frac{\sigma_X}{\sqrt{n}}\sqrt{Q_t} \end{aligned}\right\} \tag{23}$$

The RL performance of the GWMA chart in the Shewhart-GWMA depends on the suitable choices of α and q. With $q > 0.5$ and $0.5 \leq \alpha \leq 0.90$, the GWMA chart outperforms the EWMA chart when detecting small shifts. The GWMA chart reduces to the EWMA chart for $\alpha = 1$ and $q = 1 - \lambda$, where $\lambda \in (0, 1]$ is the smoothing constant of the EWMA statistic. Here, $\mathrm{L}_1(> 0)$ in Eq. (16) and $\mathrm{L}_3(> 0)$ are the control charting multiplier, and their values are selected so that the IC ARL of the Shewhart-GWMA chart reaches the desired level. Note that the UCL and LCLs are both time-varying. The Shewhart-GWMA chart issues an OC signal whenever $H_t > UCL_t$ or $H_t < LCL_t$, or $\overline{X}_t > UCL$ or $\overline{X}_t < LCL$.

3.5. Monte Carlo simulations on the effect of measurement uncertainty

Generally, there are three methods to compute the RL properties of control charts; the Integral Equation method, the Markov Chain method, and Monte Carlo simulation; see, for instance, Park et al. (2021). Considering the complexity of the charting schemes of the studied charts in this paper, we perform Monte Carlo simulations to evaluate the RL, especially ARL profiles of different charts with measurement uncertainty. In addition, to evaluate the overall performance of the charts, extra quadratic loss (EQL), relative ARL (RARL) and performance comparison index (PCI) are used. The detailed procedure of the Monte Carlo simulation of the measurement uncertainty-based Shewhart-CUSUM chart is summarized as follows:

(1) For a desired IC ARL, set the parameters (m, n, A, B) in the linear covariate model and choose the design parameters (L_1, k, h) with the γ (0 to 1) of the Shewhart-CUSUM chart.

(2) Generate a random sample $\overline{X}_t$ from the normal distribution with mean in Eq. (12) and variance in Eq. (13) or (14).

(3) If $\overline{X}_t$ falls outside the Shewhart control limits in Eq. (16), or the calculated $D_t^+(D_t^-)$ falls above the control limit $H = h\sigma_X/\sqrt{n}$, the process is deemed to be OC.

(4) Record the RL from the monitoring to the time t. Otherwise, repeat Steps (2) and (3) until the chart issues an OC signal and record the corresponding RL.

(5) Repeat Steps (2) to (4) 10^5 times and calculate the ARL, EQL, RARL, and PCI of these RL values.

For the other three charts studied in this paper we use an identical approach, substituting the chart parameters and control limits of the corresponding chart in Steps (1) and (3).

4. Analysis of the effect of measurement uncertainty on combined control charts

This section investigates the sensitive performance of the four considered charts in the presence of measurement errors. Without loss of generality, we set the desired ARL_0 (IC ARL) to be 370. Tables 1-4 present the ARL_1 (OC ARL) profiles of these charts for different values of measurement replications $m \in \{1,2,3,4\}$, ratios of measurement system variance to process variance $\gamma \in \{0.0, 0.1, \cdots, 1.0\}$ and shift size $\Delta \in \{0.25, 0.50, \cdots, 5.00\}$. These parameters are selected to cover a range of different size of possible shifts e.g., small-to-moderate as well as moderate-to-large, in the process mean, measurement accuracy errors and repeat measurements of each item. Moreover, Figs. 1-4 give a visual display of the detection abilities of the charts and show how multiple measurement strategy can compensate their power. We chose the chart parameters used in the simulation of ARL to satisfy the desired ARL_0 (when $\Delta = 0.00$) when no measurement error exists. From tables and figures, we can conclude the following:

It can be observed from Tables 1-4 that the ARL_1 values of the Shewhart-CUSUM, Shewhart-CCUSUM, Shewhart-EWMA and Shewhart-GWMA charts (at $m = 1$, 2, 3, and 4) decrease as the values of shift increase from 0.25 to 5.00. As expected, having fixed ARL_0, the ARL_1 is inversely proportional to the size of shift. For example, we may observe (δ, ARL_1) at $m = 1$ from Table 1 as (0.25, 256.15), (1.00, 17.13) and so on (2.00, 4.85). It can be perceived from Tables 1-4 that ARL_1 values of Shewhart-CUSUM, Shewhart-CCUSUM, Shewhart-EWMA and Shewhart-GWMA charts (at $m = 1$, 2, 3, and 4) increase as the ratio γ increases from 0 (perfect case) to 1.0 (worst case). The ARL_1 is directly proportional to the ratio γ, that is, more the measurement variation, higher the ARL_1. For example, we may observe (γ, ARL_1) from Table 1 as (0.00, 256.15), (0.30, 292.81), (0.60, 308.95), and so on (1.00, 319.48). With the increment of γ, the ARL_1 curves, all and sundry, shift upwards to the right. From Figs. 1-4, the left bottom curve is for $\gamma = 0$ and the right top most curve is for $\gamma = 1.0$.

The ARL_1 performance for different size of measurement errors on the Shewhart-CUSUM, with repeated measurements ($m \in \{2, 3, 4\}$) can also be found in Table 1. As it can be seen, measuring each item several times can increase the measurement accuracy and reduce the negative effect of measurement uncertainty on the Shewhart-CUSUM, for example one may can observe (m, ARL_1) when $\Delta = \gamma = 0.50$ as, (1, 166.50), (2, 139.05), (3, 129.33), and (4, 123.70). This improvement in detection ability of the other each chart has increase as the value of m increase from 1 to 4. Tables 3-4 demonstrate that the Shewhart-CCUSUM, Shewhart-EWMA and Shewhart-GWMA charts behave similarly regarding the negative effect of measurement uncertainty on the chart's performance respectively. Repeated measurements reduce this negative effect by performing as a remedial scheme. The tendency is supported by Figs. 1-4 as well.

In order to compare the sensitivity of the Shewhart-CUSUM and Shewhart-CCUSUM, from Tables 1-2 as well as Figs. 1-2, can be observed when $\Delta = 0.5$ at $m = 1$, both charts have the similar ARL_1 performances when $\gamma = 0$. However, comparing ARL_1 if γ increases up to 1, the former has ARL_1 performance is 220.30, respectively while later is 170.54 which show that the measurement uncertainty has a larger effect on Shewhart-CUSUM than on the Shewhart-CCUSUM chart. We can draw similar conclusions for the Shewhart-EWMA and Shewhart-GWMA charts as we drew for the Shewhart-CUSUM. Figs. 3-4 and Tables 3-4 have similar ARL_1 performance when $\gamma = 0$. If γ increases up to 1, $\mathrm{ARL}_1 = 281$ of the Shewhart-EWMA are larger than the $\mathrm{ARL}_1 = 219$ of the Shewhart-GWMA chart.

Table 5 gives the RARL, EQL, and PCI of these charts for different $m \in \{1, 2, 3, 4\}$ and $\gamma \in \{0.0, 0.1, \cdots, 1.0\}$. These measures are mathematically defined as follows:

$$\mathrm{EQL} = \frac{1}{s+1}\sum_{i=0}^{s}\delta_i{}^2\mathrm{ARL}(\delta_i), \tag{24}$$

$$\mathrm{RARL} = \frac{1}{s+1}\sum_{i=0}^{s}\frac{\mathrm{ARL_c}(\delta_i)}{\mathrm{ARL_{opt}}(\delta_i)} \tag{25}$$

and

$$\mathrm{PCI} = \mathrm{EQL}/\mathrm{EQL_{opt}} \tag{26}$$

where $\delta_i = a + i(b-a)/s$ and s is a given integer. Here, we considered the optimal classical two-sided CUSUM chart. The smaller the value of the EQL, the better the overall sensitivity of a chart will be. The RARL value is one for the optimal chart. Therefore, the more similar the given

Table 1
ARL_1 profile of the Two-sided Combined Shewhart-CUSUM Chart at m = 1, 2, 3, and 4 with $ARL_o = 370$.

							γ					
Δ	***m***	**0**	**0.1**	**0.2**	**0.3**	**0.4**	**0.5**	**0.6**	**0.7**	**0.8**	**0.9**	**1**
0.25	1	256.15	272.00	284.79	292.81	297.83	303.19	308.95	312.15	315.81	319.64	319.48
	2	257.40	268.96	276.05	283.75	288.99	293.77	296.12	298.92	302.80	304.92	305.49
	3	258.32	267.15	275.34	279.76	285.42	290.60	292.83	293.50	296.87	295.89	299.50
	4	255.60	265.06	272.43	279.48	281.72	286.44	288.27	292.23	292.74	295.02	296.93
0.50	1	80.87	96.76	114.74	132.49	150.95	166.50	179.81	194.08	204.86	212.96	220.30
	2	80.48	91.25	103.71	115.25	127.14	139.05	150.52	161.20	168.94	179.57	186.79
	3	80.77	90.16	98.84	109.03	119.34	129.33	138.29	147.73	156.34	163.64	170.80
	4	80.76	89.40	96.77	106.63	115.06	123.70	132.07	139.75	148.30	155.03	162.27
0.75	1	30.38	35.67	41.66	48.22	55.58	63.60	71.99	81.56	91.21	101.15	112.08
	2	30.38	33.79	37.70	41.66	46.06	50.74	55.47	60.76	66.39	71.94	77.46
	3	30.38	33.20	36.36	39.52	42.96	46.54	50.52	54.38	58.74	63.00	67.53
	4	30.26	33.08	35.60	38.68	41.56	44.59	47.85	51.43	54.86	58.64	62.23
1.00	1	17.13	19.71	22.52	25.48	28.83	32.47	36.27	40.52	45.19	49.69	54.82
	2	17.12	18.86	20.69	22.65	24.72	26.77	29.13	31.58	34.12	36.80	39.62
	3	17.19	18.53	20.06	21.66	23.31	25.05	26.84	28.80	30.85	32.80	35.02
	4	17.12	18.47	19.79	21.16	22.55	24.16	25.78	27.33	29.23	31.00	32.74
1.25	1	11.54	13.08	14.78	16.63	18.57	20.74	22.98	25.43	27.93	30.67	33.42
	2	11.50	12.58	13.67	14.84	16.10	17.45	18.82	20.24	21.80	23.39	25.05
	3	11.51	12.35	13.31	14.22	15.32	16.35	17.44	18.60	19.76	21.04	22.18
	4	11.47	12.30	13.10	13.99	14.83	15.80	16.69	17.66	18.76	19.82	20.85
1.50	1	8.35	9.47	10.65	11.89	13.27	14.71	16.17	17.80	19.47	21.29	23.22
	2	8.36	9.06	9.83	10.64	11.46	12.34	13.29	14.25	15.29	16.34	17.40
	3	8.35	8.93	9.58	10.16	10.87	11.58	12.30	13.04	13.85	14.58	15.46
	4	8.36	8.87	9.44	10.02	10.57	11.22	11.78	12.46	13.13	13.76	14.46
1.75	1	6.31	7.14	8.01	8.96	9.93	10.96	12.05	13.21	14.40	15.73	17.09
	2	6.31	6.84	7.35	7.93	8.50	9.22	9.82	10.49	11.22	11.94	12.71
	3	6.30	6.72	7.17	7.61	8.07	8.56	9.06	9.58	10.12	10.68	11.23
	4	6.31	6.65	7.06	7.41	7.84	8.24	8.67	9.10	9.53	9.98	10.44
2.00	1	4.85	5.49	6.16	6.89	7.62	8.43	9.25	10.10	11.05	11.96	12.99
	2	4.86	5.24	5.64	6.05	6.52	6.96	7.42	7.94	8.41	8.98	9.49
	3	4.86	5.14	5.45	5.80	6.10	6.45	6.80	7.16	7.55	7.91	8.30
	4	4.85	5.11	5.36	5.65	5.90	6.21	6.49	6.81	7.06	7.36	7.71
2.25	1	3.81	4.30	4.81	5.38	5.98	6.58	7.18	7.91	8.59	9.29	10.10
	2	3.78	4.07	4.37	4.69	5.01	5.35	5.68	6.07	6.44	6.81	7.21
	3	3.78	4.00	4.23	4.44	4.68	4.94	5.19	5.45	5.69	5.95	6.23
	4	3.78	3.96	4.15	4.34	4.53	4.73	4.92	5.13	5.32	5.53	5.74
2.50	1	2.99	3.38	3.78	4.22	4.69	5.18	5.66	6.19	6.74	7.33	7.93
	2	2.99	3.20	3.42	3.66	3.90	4.15	4.42	4.69	4.97	5.25	5.52
	3	3.00	3.14	3.29	3.48	3.64	3.82	3.98	4.17	4.36	4.55	4.73
	4	3.00	3.11	3.24	3.37	3.50	3.65	3.77	3.91	4.08	4.19	4.35
2.75	1	2.41	2.71	3.04	3.37	3.74	4.11	4.51	4.93	5.37	5.80	6.26
	2	2.41	2.56	2.72	2.90	3.07	3.26	3.45	3.68	3.87	4.08	4.28
	3	2.41	2.52	2.63	2.75	2.86	3.00	3.12	3.25	3.39	3.52	3.66
	4	2.40	2.50	2.58	2.68	2.77	2.85	2.96	3.06	3.16	3.26	3.35
3.00	1	1.97	2.20	2.46	2.73	2.99	3.29	3.63	3.93	4.29	4.64	5.00
	2	1.97	2.09	2.22	2.34	2.49	2.63	2.76	2.92	3.07	3.22	3.39
	3	1.97	2.05	2.13	2.22	2.30	2.40	2.48	2.58	2.69	2.79	2.89
	4	1.96	2.04	2.10	2.16	2.24	2.31	2.35	2.44	2.51	2.58	2.65
3.50	1	1.45	1.58	1.73	1.89	2.06	2.23	2.44	2.63	2.84	3.07	3.28
	2	1.44	1.51	1.58	1.66	1.73	1.81	1.89	1.98	2.07	2.15	2.24
	3	1.44	1.49	1.53	1.58	1.63	1.68	1.73	1.79	1.85	1.90	1.95
	4	1.44	1.47	1.51	1.55	1.58	1.62	1.66	1.70	1.73	1.77	1.81
4.00	1	1.19	1.26	1.35	1.44	1.54	1.65	1.77	1.90	2.03	2.17	2.30
	2	1.19	1.23	1.26	1.30	1.35	1.39	1.44	1.49	1.54	1.59	1.66
	3	1.19	1.21	1.24	1.26	1.29	1.32	1.35	1.38	1.41	1.44	1.47
	4	1.19	1.21	1.22	1.25	1.26	1.28	1.30	1.32	1.35	1.37	1.39
5.00	1	1.02	1.04	1.06	1.09	1.12	1.16	1.21	1.25	1.30	1.36	1.42
	2	1.02	1.03	1.04	1.05	1.06	1.08	1.09	1.11	1.12	1.14	1.16
	3	1.02	1.03	1.03	1.04	1.05	1.05	1.06	1.07	1.08	1.09	1.10
	4	1.02	1.03	1.03	1.04	1.04	1.04	1.05	1.06	1.06	1.07	1.08

Table 2
ARL_1 profile of the Two-sided Combined Shewhart-CCUSUM Chart at m = 1, 2, 3, and 4 with $ARL_o = 370$.

		γ										
Δ	***m***	**0**	**0.1**	**0.2**	**0.3**	**0.4**	**0.5**	**0.6**	**0.7**	**0.8**	**0.9**	**1**
0.25	1	255.41	264.36	271.65	278.20	286.24	291.26	296.93	299.60	303.60	307.07	311.76
	2	256.94	260.06	264.56	269.35	274.27	276.35	278.51	282.21	286.17	287.82	291.66
	3	255.78	257.69	263.05	264.06	267.27	270.15	273.64	276.66	276.65	281.36	283.85
	4	255.68	257.19	261.43	263.37	264.54	266.33	271.17	271.71	274.26	273.74	278.53
0.50	1	79.86	90.15	100.00	109.97	119.25	129.01	137.81	146.37	154.22	161.98	170.54
	2	80.13	85.23	90.24	95.39	100.20	105.51	110.30	114.51	119.58	124.05	129.20
	3	80.37	83.14	86.66	89.83	93.55	96.50	100.25	103.53	106.64	109.61	113.04
	4	80.16	82.22	84.95	87.55	90.28	92.53	95.21	97.14	100.64	102.62	104.92
0.75	1	29.97	33.52	36.99	40.36	44.31	48.22	52.19	55.99	60.51	64.96	69.10
	2	30.13	31.73	33.41	35.03	36.75	38.58	40.53	42.21	44.16	46.27	48.16
	3	30.02	31.14	32.30	33.46	34.52	35.74	36.94	37.98	39.23	40.50	41.65
	4	30.19	30.85	31.71	32.53	33.39	34.18	35.21	36.09	36.87	37.63	38.50
1.00	1	16.90	18.51	20.07	21.76	23.42	25.11	26.93	28.69	30.53	32.37	34.13
	2	16.94	17.73	18.49	19.26	20.07	20.92	21.76	22.57	23.44	24.28	25.03
	3	16.94	17.45	17.96	18.50	19.07	19.57	20.16	20.60	21.19	21.73	22.36
	4	16.94	17.28	17.71	18.13	18.51	18.84	19.34	19.67	20.10	20.57	20.95
1.25	1	11.35	12.38	13.35	14.29	15.35	16.27	17.31	18.37	19.36	20.38	21.41
	2	11.36	11.87	12.33	12.82	13.36	13.85	14.34	14.84	15.36	15.77	16.33
	3	11.34	11.71	12.02	12.34	12.68	13.00	13.35	13.71	14.01	14.31	14.67
	4	11.41	11.59	11.85	12.09	12.40	12.58	12.86	13.09	13.34	13.56	13.82
1.50	1	8.25	8.97	9.69	10.38	11.10	11.81	12.45	13.16	13.81	14.52	15.23
	2	8.23	8.64	8.95	9.32	9.72	10.03	10.39	10.75	11.08	11.43	11.77
	3	8.23	8.48	8.72	8.96	9.24	9.46	9.71	9.92	10.15	10.39	10.63
	4	8.24	8.44	8.62	8.79	8.97	9.13	9.33	9.53	9.70	9.82	10.02
1.75	1	6.24	6.81	7.37	7.92	8.47	8.96	9.52	10.00	10.51	11.02	11.54
	2	6.24	6.54	6.82	7.09	7.37	7.65	7.90	8.17	8.44	8.70	9.00
	3	6.23	6.45	6.62	6.83	7.00	7.20	7.38	7.58	7.76	7.92	8.09
	4	6.23	6.39	6.52	6.65	6.81	6.95	7.08	7.24	7.38	7.53	7.64
2.00	1	4.81	5.29	5.74	6.22	6.66	7.10	7.52	7.91	8.34	8.76	9.17
	2	4.81	5.08	5.31	5.52	5.76	6.00	6.21	6.42	6.66	6.87	7.10
	3	4.81	4.98	5.13	5.31	5.46	5.61	5.76	5.93	6.06	6.23	6.36
	4	4.82	4.94	5.05	5.16	5.29	5.41	5.55	5.64	5.76	5.86	5.96
2.25	1	3.77	4.19	4.56	4.94	5.32	5.69	6.06	6.40	6.75	7.11	7.43
	2	3.76	3.97	4.17	4.37	4.55	4.75	4.95	5.15	5.33	5.52	5.70
	3	3.76	3.92	4.03	4.17	4.29	4.44	4.56	4.70	4.81	4.96	5.07
	4	3.76	3.87	3.97	4.07	4.16	4.26	4.37	4.47	4.57	4.67	4.76
2.50	1	2.98	3.31	3.65	3.97	4.31	4.61	4.93	5.23	5.53	5.82	6.13
	2	2.97	3.15	3.33	3.48	3.66	3.81	3.97	4.15	4.31	4.47	4.63
	3	2.98	3.08	3.21	3.32	3.43	3.55	3.64	3.76	3.87	3.98	4.09
	4	2.99	3.07	3.15	3.24	3.33	3.40	3.49	3.56	3.65	3.74	3.81
2.75	1	2.40	2.68	2.96	3.22	3.51	3.78	4.06	4.31	4.59	4.83	5.10
	2	2.39	2.53	2.67	2.81	2.96	3.09	3.23	3.37	3.50	3.66	3.78
	3	2.40	2.49	2.57	2.69	2.76	2.86	2.95	3.04	3.14	3.23	3.33
	4	2.40	2.46	2.53	2.60	2.68	2.75	2.82	2.88	2.95	3.01	3.10
3.00	1	1.97	2.20	2.42	2.66	2.89	3.12	3.35	3.58	3.82	4.04	4.27
	2	1.96	2.08	2.19	2.31	2.43	2.53	2.65	2.77	2.88	3.01	3.14
	3	1.97	2.04	2.11	2.19	2.26	2.35	2.42	2.50	2.57	2.65	2.74
	4	1.97	2.02	2.08	2.13	2.18	2.25	2.31	2.35	2.41	2.48	2.54
3.50	1	1.45	1.57	1.73	1.87	2.03	2.20	2.36	2.54	2.70	2.88	3.05
	2	1.45	1.51	1.58	1.65	1.71	1.79	1.87	1.95	2.03	2.10	2.20
	3	1.44	1.49	1.53	1.57	1.62	1.68	1.72	1.77	1.82	1.87	1.93
	4	1.45	1.48	1.51	1.54	1.58	1.61	1.65	1.68	1.72	1.76	1.80
4.00	1	1.19	1.26	1.35	1.44	1.54	1.65	1.77	1.87	2.00	2.12	2.25
	2	1.19	1.23	1.26	1.30	1.34	1.39	1.44	1.48	1.54	1.58	1.65
	3	1.19	1.21	1.24	1.26	1.29	1.31	1.34	1.37	1.41	1.44	1.47
	4	1.19	1.21	1.23	1.25	1.26	1.28	1.30	1.32	1.35	1.37	1.39
5.00	1	1.02	1.04	1.06	1.09	1.12	1.16	1.21	1.25	1.31	1.37	1.42
	2	1.02	1.03	1.04	1.05	1.06	1.08	1.09	1.11	1.12	1.14	1.16
	3	1.02	1.03	1.03	1.04	1.05	1.05	1.06	1.07	1.08	1.09	1.10
	4	1.02	1.03	1.03	1.04	1.04	1.04	1.05	1.06	1.06	1.07	1.08

Table 3
ARL_1 profile of the Two-sided Combined Shewhart-EWMA Chart at $m = 1, 2, 3$, and 4 with $ARL_o = 370$.

							γ				
Δ	***m***	**0**	**0.1**	**0.2**	**0.3**	**0.4**	**0.5**	**0.6**	**0.7**	**0.8**	**0.9**	**1**
0.25	1	280.28	294.06	304.22	312.36	317.19	324.46	330.32	335.78	337.73	340.88	343.05
	2	281.67	291.69	300.97	306.24	310.98	317.15	321.64	326.28	329.21	332.22	334.11
	3	281.87	287.87	297.26	303.66	308.21	314.85	317.55	322.95	327.12	330.46	329.63
	4	281.31	288.52	296.04	301.49	308.41	312.26	316.67	320.44	324.62	327.71	328.54
0.50	1	155.74	174.71	192.21	207.13	221.54	235.82	245.93	257.59	265.21	275.51	280.56
	2	155.39	169.61	183.69	195.42	208.03	218.00	227.64	237.13	244.61	252.07	259.59
	3	155.41	168.42	180.78	192.41	201.20	212.13	220.51	228.03	235.84	244.19	249.90
	4	154.90	166.92	178.57	189.00	199.23	206.56	215.19	223.30	230.69	237.53	243.69
0.75	1	80.74	96.90	111.93	126.99	142.53	155.97	168.72	180.43	191.24	202.46	212.28
	2	81.19	92.69	104.65	115.22	126.02	137.39	148.09	157.60	165.91	176.57	184.36
	3	81.13	91.63	101.74	111.53	121.55	130.82	139.32	147.80	156.34	163.58	172.55
	4	81.17	90.63	100.21	109.81	118.00	126.84	135.20	144.17	151.22	158.68	164.99
1.00	1	43.95	54.58	65.58	76.72	89.02	101.02	111.81	123.73	133.94	144.84	154.87
	2	43.98	51.80	60.13	68.51	76.72	85.55	94.26	102.01	110.85	118.45	127.12
	3	44.15	50.95	58.17	65.54	72.53	80.13	87.36	94.19	101.97	108.82	115.30
	4	43.80	50.37	57.10	64.14	70.56	77.40	84.13	90.31	97.11	103.75	110.14
1.25	1	24.90	32.01	39.98	48.31	57.21	65.56	75.04	84.58	93.55	103.00	111.81
	2	24.87	30.29	35.88	41.50	47.69	54.45	60.38	67.08	74.36	80.70	87.20
	3	24.93	29.53	34.37	39.45	44.53	49.73	55.67	60.83	66.48	72.76	78.44
	4	24.98	29.30	33.85	38.38	43.28	47.98	53.07	57.90	63.21	68.11	73.59
1.50	1	14.94	19.61	24.99	30.90	37.16	43.86	50.78	58.69	66.04	73.13	80.84
	2	14.95	18.35	22.19	26.22	30.55	35.28	40.11	44.88	50.22	55.47	60.75
	3	14.96	17.98	21.35	24.70	28.36	32.08	36.38	40.41	44.56	49.01	53.39
	4	15.00	17.85	20.88	23.98	27.24	30.73	34.50	38.13	41.87	45.75	49.60
1.75	1	9.44	12.58	16.14	20.46	24.81	29.72	35.26	41.00	46.89	53.28	59.28
	2	9.48	11.73	14.38	17.23	20.23	23.47	27.07	30.66	34.64	38.51	42.76
	3	9.46	11.46	13.61	16.00	18.57	21.26	24.37	27.24	30.41	33.77	37.23
	4	9.45	11.37	13.35	15.60	17.87	20.29	22.86	25.58	28.21	31.08	34.46
2.00	1	6.30	8.46	10.96	13.96	17.22	20.85	24.91	29.30	34.06	38.76	43.88
	2	6.29	7.88	9.63	11.65	13.91	16.17	18.72	21.50	24.37	27.57	30.64
	3	6.32	7.68	9.19	10.81	12.71	14.75	16.85	18.95	21.31	23.90	26.40
	4	6.30	7.57	8.94	10.51	12.13	13.92	15.75	17.68	19.82	21.92	24.21
2.25	1	4.43	5.89	7.68	9.77	12.29	15.05	17.95	21.35	24.99	28.85	32.77
	2	4.41	5.48	6.72	8.10	9.65	11.45	13.38	15.39	17.60	20.00	22.42
	3	4.42	5.37	6.41	7.57	8.90	10.30	11.80	13.55	15.20	17.17	19.12
	4	4.38	5.28	6.23	7.33	8.57	9.75	11.16	12.57	14.13	15.62	17.46
2.50	1	3.24	4.30	5.59	7.10	8.90	10.96	13.31	15.76	18.66	21.68	24.97
	2	3.25	4.00	4.89	5.91	7.01	8.29	9.74	11.31	13.00	14.76	16.79
	3	3.24	3.90	4.67	5.51	6.45	7.51	8.64	9.83	11.18	12.60	14.06
	4	3.24	3.85	4.53	5.31	6.17	7.12	8.06	9.19	10.29	11.53	12.81
2.75	1	2.48	3.25	4.17	5.33	6.65	8.22	9.96	11.99	14.18	16.57	19.14
	2	2.50	3.03	3.68	4.42	5.25	6.23	7.26	8.45	9.73	11.13	12.70
	3	2.49	2.96	3.51	4.13	4.83	5.59	6.45	7.36	8.37	9.40	10.67
	4	2.49	2.93	3.43	4.00	4.64	5.33	6.03	6.83	7.72	8.65	9.66
3.00	1	2.00	2.54	3.24	4.10	5.12	6.29	7.68	9.23	10.99	12.91	14.93
	2	2.00	2.40	2.86	3.43	4.07	4.81	5.58	6.48	7.50	8.60	9.76
	3	2.01	2.35	2.75	3.22	3.72	4.31	4.95	5.66	6.41	7.24	8.13
	4	2.00	2.32	2.68	3.11	3.58	4.07	4.65	5.26	5.95	6.64	7.43
3.50	1	1.45	1.75	2.14	2.64	3.26	3.96	4.82	5.77	6.86	8.09	9.51
	2	1.45	1.66	1.93	2.25	2.62	3.03	3.55	4.08	4.69	5.35	6.10
	3	1.45	1.63	1.87	2.12	2.43	2.78	3.14	3.58	4.05	4.57	5.14
	4	1.45	1.62	1.83	2.07	2.33	2.63	2.96	3.33	3.72	4.16	4.62
4.00	1	1.19	1.35	1.59	1.88	2.25	2.71	3.25	3.85	4.57	5.35	6.33
	2	1.19	1.31	1.46	1.65	1.87	2.13	2.44	2.79	3.16	3.61	4.07
	3	1.19	1.30	1.42	1.57	1.76	1.96	2.20	2.47	2.76	3.08	3.44
	4	1.19	1.29	1.40	1.53	1.70	1.89	2.09	2.32	2.55	2.84	3.11
5.00	1	1.02	1.06	1.14	1.25	1.40	1.58	1.82	2.10	2.42	2.80	3.24
	2	1.02	1.05	1.10	1.16	1.24	1.35	1.47	1.62	1.79	1.98	2.21
	3	1.02	1.05	1.08	1.13	1.20	1.28	1.37	1.48	1.61	1.75	1.91
	4	1.02	1.05	1.08	1.12	1.18	1.25	1.33	1.42	1.52	1.65	1.78

chart is to the optimum chart, the closer the RARL value is to unity. PCI is the ratio of a chart's EQL to the EQL of the best chart under the same conditions. This index makes it easier to compare performances by completing ranking based on EQL.

As Table 5 shows, the RARL, EQL and PCI of the four combined charts increases as the measurement error γ increases. By repeating measurements, the RARL, EQL and PCI decrease when measurement error occurs. The EQL values are interpreted similarly to ARL_1. For instance, one

Table 4
ARL_1 profile of the Two-sided Combined Shewhart-GWMA Chart at $m = 1$, 2, 3, and 4 with $ARL_o = 370$.

		γ										
Δ	***m***	**0**	**0.1**	**0.2**	**0.3**	**0.4**	**0.5**	**0.6**	**0.7**	**0.8**	**0.9**	**1**
0.25	1	277.54	284.55	291.91	295.77	300.09	304.23	308.65	311.02	312.60	315.46	320.37
	2	279.31	281.18	288.09	287.20	291.77	293.86	295.09	297.90	300.57	302.59	305.17
	3	280.70	281.80	283.19	286.01	287.12	290.29	291.43	291.31	295.30	297.75	298.11
	4	278.96	282.50	282.15	282.63	285.28	286.79	289.52	291.26	290.46	290.02	291.75
0.50	1	147.30	158.76	167.42	175.77	183.73	191.53	197.62	202.74	208.72	214.66	219.14
	2	149.05	153.14	157.85	162.91	167.82	171.10	176.58	179.02	183.88	187.34	190.80
	3	148.34	151.27	154.77	158.68	160.74	164.72	166.47	170.44	172.94	176.08	178.74
	4	148.02	150.74	153.58	155.86	158.34	161.25	163.19	165.01	167.49	169.25	171.48
0.75	1	70.40	78.43	85.69	93.25	99.83	106.55	112.87	119.19	124.67	130.74	134.91
	2	70.52	74.11	78.19	82.12	86.10	89.62	93.61	96.42	100.57	103.33	106.91
	3	70.50	73.05	75.58	78.14	80.85	83.17	86.11	88.71	90.48	93.21	95.15
	4	70.85	72.43	74.38	76.15	78.32	80.25	82.18	83.91	85.85	87.32	89.56
1.00	1	34.40	38.97	43.85	48.48	53.39	58.23	62.71	67.23	71.91	75.81	80.44
	2	34.24	36.64	39.26	41.50	43.90	46.12	48.38	50.72	53.17	55.53	58.14
	3	34.30	35.86	37.45	38.72	40.67	42.09	43.46	45.46	46.82	48.20	49.93
	4	34.40	35.59	36.59	37.85	38.92	40.28	41.22	42.39	43.54	44.85	46.04
1.25	1	18.53	21.12	23.75	26.60	29.67	32.53	35.37	38.09	41.41	44.44	47.45
	2	18.59	19.72	21.13	22.53	23.84	25.24	26.64	27.95	29.51	30.95	32.29
	3	18.46	19.38	20.18	21.13	22.06	22.85	23.83	24.74	25.60	26.75	27.67
	4	18.52	19.07	19.83	20.43	21.05	21.82	22.50	23.08	23.78	24.57	25.20
1.50	1	11.18	12.70	14.36	16.06	17.83	19.61	21.40	23.33	25.16	27.19	29.29
	2	11.18	11.98	12.65	13.55	14.34	15.16	16.03	16.92	17.73	18.69	19.58
	3	11.17	11.70	12.23	12.74	13.29	13.83	14.32	14.94	15.47	16.10	16.62
	4	11.19	11.56	11.93	12.34	12.73	13.16	13.54	13.94	14.34	14.82	15.27
1.75	1	7.39	8.37	9.44	10.51	11.57	12.78	13.88	15.10	16.40	17.65	19.06
	2	7.39	7.86	8.36	8.89	9.40	9.95	10.46	11.11	11.62	12.15	12.80
	3	7.41	7.72	8.05	8.36	8.72	9.06	9.42	9.78	10.19	10.51	10.86
	4	7.35	7.64	7.89	8.13	8.40	8.65	8.87	9.16	9.44	9.70	9.97
2.00	1	5.21	5.90	6.61	7.33	8.07	8.87	9.69	10.45	11.37	12.27	13.10
	2	5.22	5.55	5.90	6.24	6.63	6.97	7.37	7.72	8.12	8.51	8.87
	3	5.22	5.44	5.66	5.91	6.12	6.36	6.59	6.83	7.13	7.33	7.57
	4	5.21	5.38	5.55	5.74	5.87	6.08	6.24	6.45	6.63	6.79	7.00
2.25	1	3.85	4.35	4.87	5.38	5.95	6.49	7.08	7.67	8.30	8.92	9.54
	2	3.85	4.11	4.34	4.63	4.86	5.14	5.41	5.66	5.95	6.22	6.52
	3	3.86	4.00	4.19	4.34	4.52	4.68	4.87	5.04	5.21	5.38	5.57
	4	3.84	3.96	4.10	4.22	4.37	4.47	4.60	4.74	4.85	4.97	5.11
2.50	1	2.96	3.34	3.72	4.10	4.55	4.96	5.36	5.80	6.24	6.72	7.21
	2	2.96	3.15	3.33	3.54	3.73	3.90	4.11	4.33	4.51	4.75	4.95
	3	2.96	3.09	3.20	3.33	3.45	3.58	3.72	3.86	3.98	4.11	4.25
	4	2.95	3.07	3.14	3.24	3.33	3.42	3.54	3.61	3.73	3.83	3.91
2.75	1	2.37	2.65	2.93	3.25	3.56	3.88	4.21	4.55	4.88	5.24	5.60
	2	2.36	2.50	2.64	2.79	2.93	3.08	3.23	3.40	3.56	3.70	3.87
	3	2.36	2.46	2.55	2.64	2.75	2.85	2.95	3.03	3.14	3.24	3.33
	4	2.36	2.43	2.50	2.57	2.65	2.72	2.80	2.87	2.94	3.02	3.09
3.00	1	1.94	2.17	2.38	2.62	2.87	3.11	3.37	3.64	3.92	4.20	4.49
	2	1.94	2.05	2.16	2.28	2.38	2.51	2.62	2.75	2.87	3.00	3.12
	3	1.94	2.02	2.08	2.16	2.23	2.32	2.38	2.47	2.55	2.61	2.71
	4	1.94	1.99	2.06	2.10	2.15	2.22	2.26	2.33	2.39	2.44	2.50
3.25	1	1.64	1.81	1.99	2.19	2.37	2.57	2.78	2.99	3.22	3.44	3.66
	2	1.65	1.73	1.81	1.90	1.99	2.08	2.17	2.27	2.37	2.47	2.57
	3	1.64	1.70	1.76	1.81	1.87	1.93	1.99	2.05	2.11	2.17	2.24
	4	1.64	1.69	1.73	1.77	1.81	1.86	1.90	1.95	1.99	2.03	2.08
3.50	1	1.44	1.57	1.70	1.84	2.01	2.17	2.32	2.51	2.68	2.85	3.04
	2	1.44	1.50	1.57	1.64	1.70	1.78	1.85	1.92	2.00	2.08	2.16
	3	1.44	1.48	1.52	1.56	1.61	1.65	1.70	1.75	1.80	1.85	1.89
	4	1.44	1.47	1.50	1.53	1.57	1.60	1.63	1.66	1.70	1.74	1.77
4.00	1	1.18	1.26	1.34	1.43	1.53	1.63	1.74	1.86	1.96	2.10	2.22
	2	1.29	1.33	1.39	1.44	1.50	1.55	1.61	1.67	1.73	1.80	1.86
	3	1.19	1.21	1.23	1.26	1.29	1.31	1.34	1.37	1.40	1.43	1.46
	4	1.19	1.21	1.22	1.24	1.26	1.28	1.30	1.32	1.34	1.37	1.39
5.00	1	1.02	1.04	1.06	1.09	1.12	1.16	1.20	1.25	1.30	1.36	1.42
	2	1.02	1.03	1.04	1.05	1.06	1.08	1.09	1.10	1.12	1.14	1.16
	3	1.02	1.03	1.03	1.04	1.05	1.05	1.06	1.07	1.08	1.09	1.10
	4	1.02	1.03	1.03	1.04	1.04	1.05	1.05	1.06	1.06	1.07	1.07

could see (γ, EQL), from Table 5 at $m = 1$ as, (0.00, 18.86), (0.30, 25.55), (0.60, 33.48) and so on (1.00, 45.76). It may also be noted that (at $\gamma = 0.70$, $m = 1$, 2, 3, 4) the respective EQL values for Shewhart-CUSUM are 36.41, 29.09, 26.17, and 24.95; for Shewhart-CCUSUM, are 30.57, 24.52, 22.58, and 21.59; for Shewhart-EWMA, are 87.83, 66.89, 60.12, and 56.88 for Shewhart-GWMA, are 40.54, 31.57, 28.75, and 26.74. This observation is similar with the other charts.

Based on the simulations results, all the studied charts significantly damage their sensitivity for detecting a shift in the process mean. The Shewhart-CUSUM is worse than the Shewhart-CCUSUM's, and the overall performance of the Shewhart-EWMA is worse than the Shewhart-GWMA's. Sensitivity based preference, Shewhart-CCUSUM uniformly and substantially outperforms than followed by the charts in the presence of measurement uncertainty.

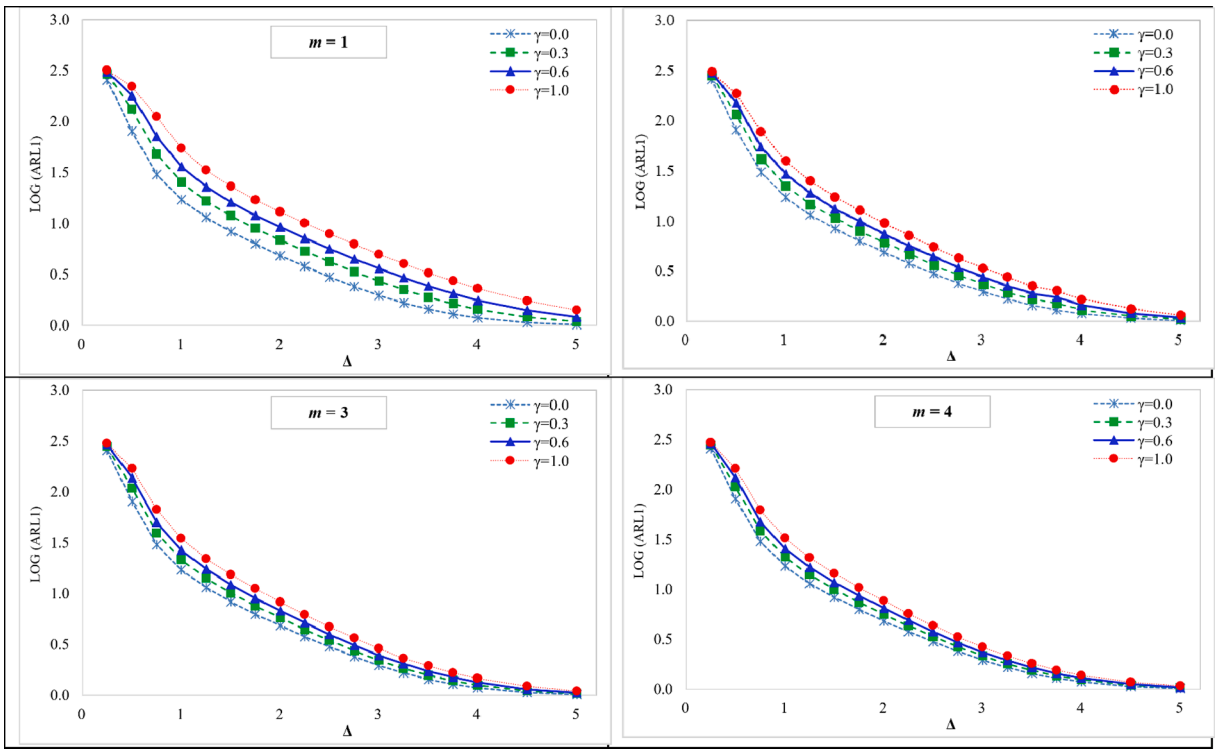

Fig. 1. Comparisons of the ARL curves of the Shewhart-CUSUM chart when $m = 1, m = 2, m = 3$ and $m = 4$

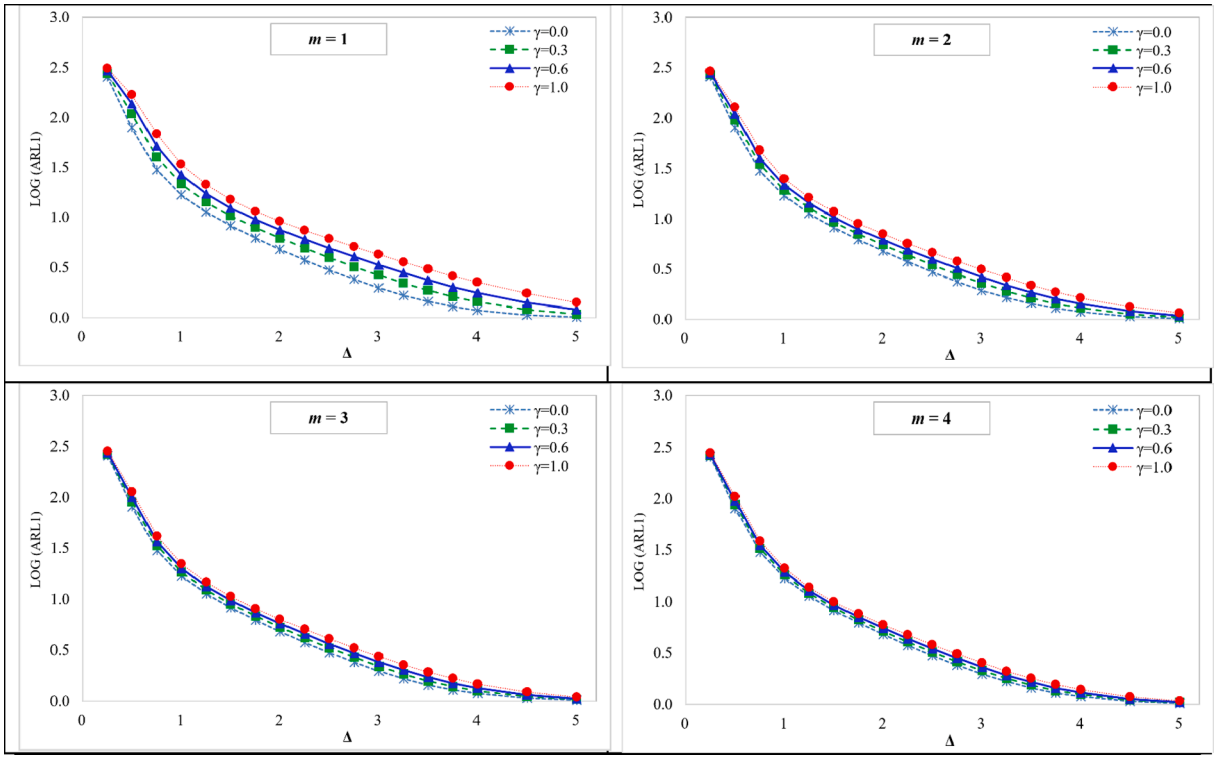

Fig. 2. Comparisons of the *ARL* curves of the Shewhart-CCUSUM chart when $m = 1, m = 2, m = 3$ and $m = 4$.

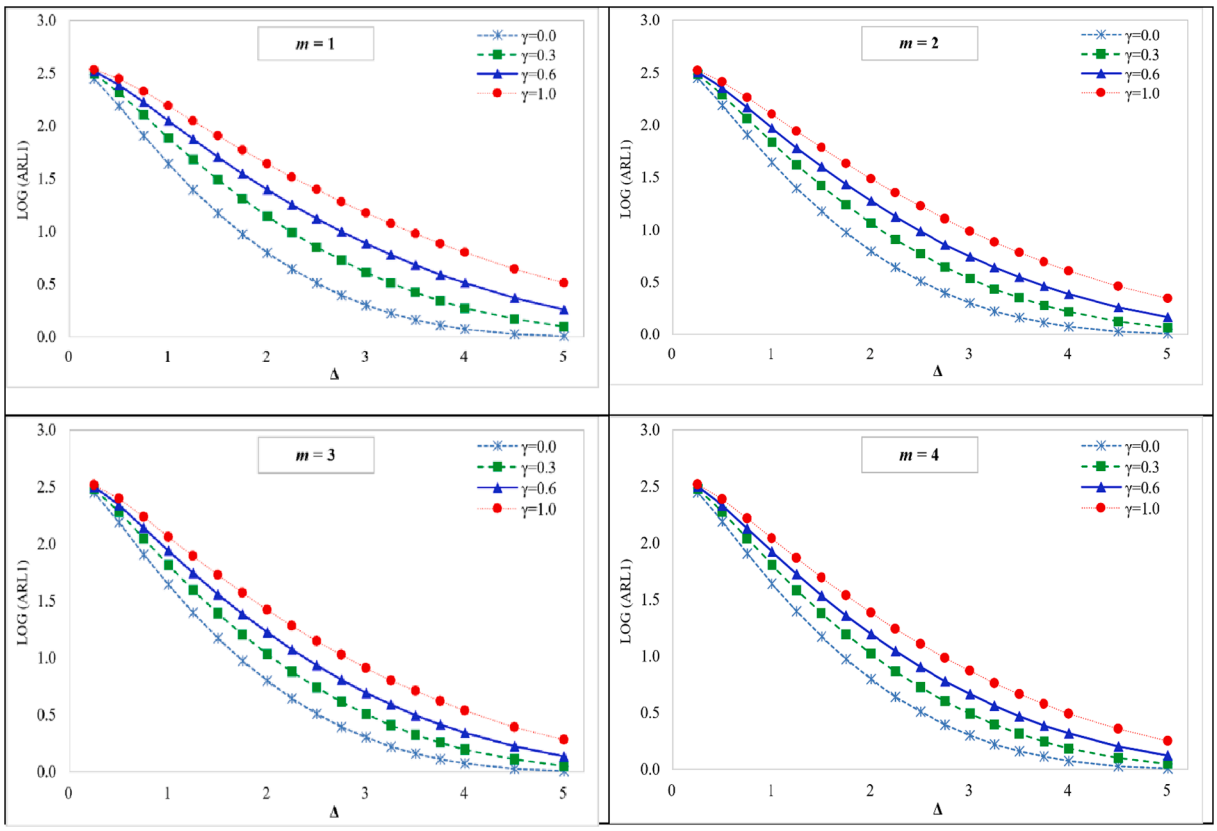

Fig. 3. Comparisons of the *ARL* curves of the Shewhart-EWMA chart when$m = 1, m = 2, m = 3$and $m = 4$.

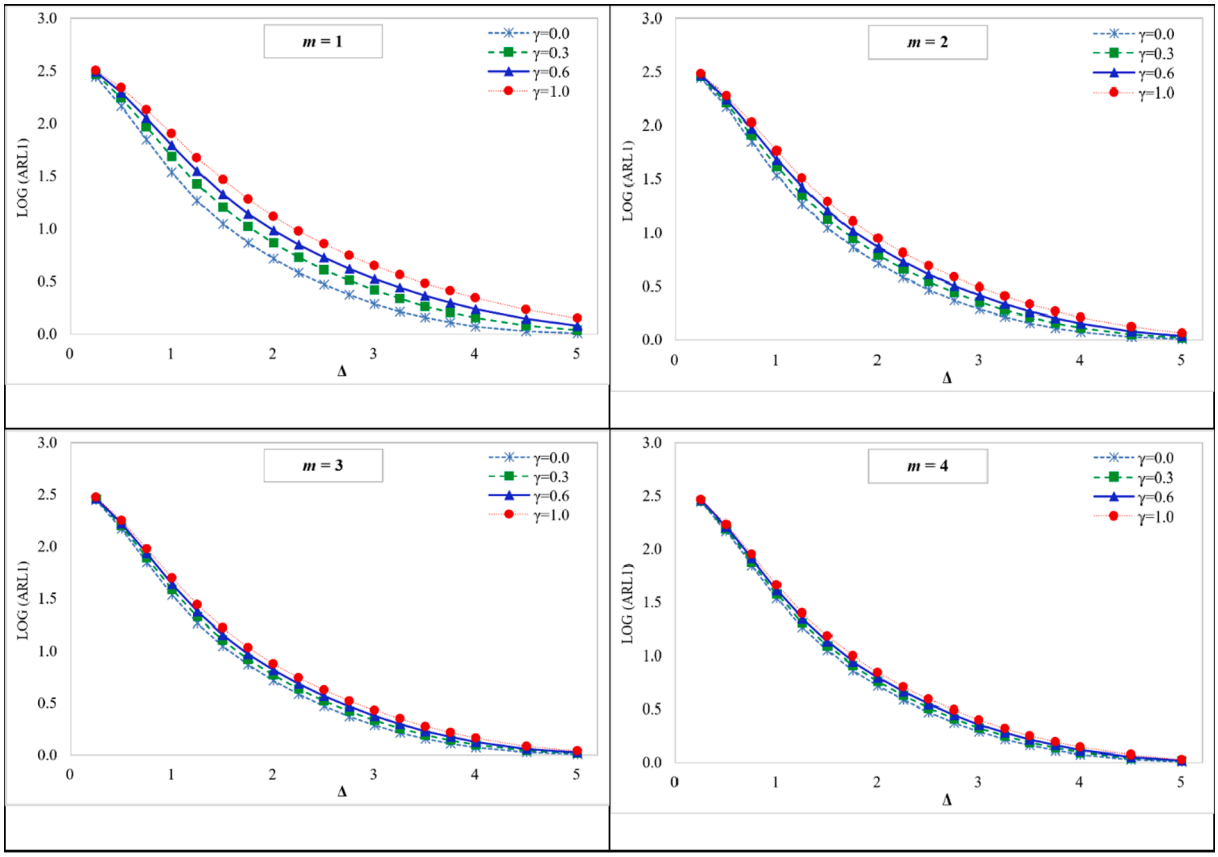

Fig. 4. Comparisons of the *ARL* curves of the Shewhart-GWMA chart when $m = 1, m = 2, m = 3$ and $m = 4$.

Table 5
RARL, EQL, and PCI performance comparisons of different charts at $m = 1$, 2, 3, and 4.

m	Chart	γ→	0	0.1	0.2	0.3	0.4	0.5	0.6	0.7	0.8	0.9	1
1	SC	RARL	1.53	1.71	1.90	2.10	2.32	2.54	2.76	3.00	3.25	3.50	3.75
		EQL	18.86	20.93	23.16	25.55	28.08	30.72	33.48	36.41	39.43	42.53	45.76
		PCI	1.34	1.48	1.64	1.81	1.99	2.18	2.37	2.58	2.80	3.02	3.25
	SCC	RARL	1.52	1.65	1.78	1.92	2.05	2.19	2.33	2.46	2.60	2.73	2.87
		EQL	18.75	20.37	22.02	23.67	25.40	27.12	28.88	30.57	32.36	34.12	35.92
		PCI	1.33	1.44	1.56	1.68	1.80	1.92	2.05	2.17	2.30	2.42	2.55
	SE	RARL	2.29	2.78	3.34	3.96	4.65	5.38	6.17	7.05	7.93	8.90	9.90
		EQL	26.21	32.12	38.98	46.82	55.68	65.36	75.72	87.83	99.84	113.69	127.89
		PCI	1.86	2.28	2.76	3.32	3.95	4.64	5.37	6.23	7.08	8.06	9.07
	SG	RARL	2.01	2.21	2.41	2.62	2.82	3.03	3.24	3.44	3.66	3.87	4.08
		EQL	23.24	25.57	27.91	30.36	32.87	35.43	37.95	40.54	43.22	45.96	48.66
		PCI	1.65	1.81	1.98	2.15	2.33	2.51	2.69	2.88	3.07	3.26	3.45
2	SC	RARL	1.53	1.64	1.76	1.88	2.01	2.14	2.27	2.42	2.55	2.70	2.84
		EQL	18.85	20.12	21.46	22.87	24.33	25.88	27.42	29.09	30.72	32.45	34.19
		PCI	1.34	1.43	1.52	1.62	1.73	1.84	1.94	2.06	2.18	2.30	2.42
	SCC	RARL	1.52	1.58	1.65	1.71	1.78	1.85	1.92	1.98	2.05	2.12	2.19
		EQL	18.75	19.57	20.37	21.17	22.01	22.84	23.69	24.52	25.40	26.24	27.16
		PCI	1.33	1.39	1.44	1.50	1.56	1.62	1.68	1.74	1.80	1.86	1.93
	SE	RARL	2.29	2.65	3.05	3.47	3.93	4.43	4.95	5.50	6.08	6.69	7.32
		EQL	26.23	30.54	35.40	40.66	46.47	52.86	59.67	66.89	74.77	82.95	91.66
		PCI	1.86	2.17	2.51	2.88	3.30	3.75	4.23	4.74	5.30	5.88	6.50
	SG	RARL	2.02	2.11	2.21	2.31	2.42	2.51	2.62	2.72	2.82	2.93	3.03
		EQL	23.28	24.38	25.56	26.77	27.94	29.13	30.36	31.57	32.87	34.11	35.41
		PCI	1.65	1.73	1.81	1.90	1.98	2.07	2.15	2.24	2.33	2.42	2.51
3	SC	RARL	1.53	1.61	1.70	1.80	1.89	1.99	2.09	2.19	2.29	2.39	2.50
		EQL	18.86	19.80	20.78	21.80	22.85	23.94	25.03	26.17	27.36	28.49	29.67
		PCI	1.34	1.40	1.47	1.55	1.62	1.70	1.78	1.86	1.94	2.02	2.10
	SCC	RARL	1.52	1.56	1.60	1.65	1.69	1.74	1.78	1.83	1.87	1.92	1.97
		EQL	18.75	19.29	19.83	20.37	20.91	21.46	22.01	22.58	23.12	23.70	24.27
		PCI	1.33	1.37	1.41	1.44	1.48	1.52	1.56	1.60	1.64	1.68	1.72
	SE	RARL	2.29	2.61	2.95	3.32	3.70	4.11	4.55	4.98	5.46	5.95	6.46
		EQL	26.25	30.03	34.18	38.66	43.51	48.74	54.36	60.12	66.35	72.98	79.88
		PCI	1.86	2.13	2.42	2.74	3.09	3.46	3.86	4.26	4.71	5.18	5.67
	SG	RARL	2.02	2.08	2.15	2.21	2.28	2.35	2.41	2.48	2.55	2.62	2.68
		EQL	23.27	24.02	24.77	25.54	26.36	27.11	27.90	28.75	29.54	30.35	31.16
		PCI	1.65	1.70	1.76	1.81	1.87	1.92	1.98	2.04	2.10	2.15	2.21
4	SC	RARL	1.52	1.60	1.68	1.76	1.84	1.92	2.00	2.09	2.17	2.26	2.34
		EQL	18.84	19.69	20.48	21.38	22.21	23.12	24.00	24.95	25.90	26.84	27.79
		PCI	1.34	1.40	1.45	1.52	1.58	1.64	1.70	1.77	1.84	1.90	1.97
	SCC	RARL	1.52	1.55	1.58	1.62	1.65	1.68	1.72	1.75	1.78	1.82	1.85
		EQL	18.78	19.16	19.56	19.96	20.37	20.75	21.20	21.59	22.02	22.42	22.84
		PCI	1.33	1.36	1.39	1.42	1.44	1.47	1.50	1.53	1.56	1.59	1.62
	SE	RARL	2.29	2.58	2.90	3.24	3.59	3.95	4.34	4.74	5.15	5.58	6.03
		EQL	26.21	29.75	33.57	37.71	42.11	46.75	51.66	56.88	62.30	68.01	74.06
		PCI	1.86	2.11	2.38	2.67	2.99	3.32	3.66	4.03	4.42	4.82	5.25
	SG	RARL	2.02	2.07	2.11	2.16	2.21	2.27	2.31	2.36	2.41	2.46	2.51
		EQL	23.26	23.84	24.41	24.97	25.55	26.18	26.74	27.33	27.92	28.51	29.13
		PCI	1.65	1.69	1.73	1.77	1.81	1.86	1.90	1.94	1.98	2.02	2.07

Note: SC - Shewhart-CUSUM; SCC - Shewhart-CCUSUM; SE - Shewhart-EWMA; and SG - Shewhart-GWMA.

Table 6
RARL, EQL, and PCI performance comparison for the covariate model with different values of *B*.

Δ	Chart	No Error	1	2	3	4	5
0.25	SC	256.15	319.48	224.62	143.79	90.55	57.95
	SCC	255.41	311.76	169.32	69.14	34.18	21.39
	SE	280.28	343.05	328.84	325.50	323.82	323.06
	SG	277.54	320.37	221.10	135.70	80.39	47.57
0.50	SC	80.87	220.30	88.78	37.95	17.79	9.16
	SCC	79.86	170.54	34.27	15.23	9.16	6.11
	SE	155.74	280.56	244.11	232.99	229.69	227.76
	SG	147.30	219.14	80.54	29.19	13.10	7.19
0.75	SC	30.38	112.08	37.41	12.59	5.25	2.76
	SCC	29.97	69.10	15.17	7.43	4.27	2.59
	SE	80.74	212.28	165.48	154.31	149.35	147.33
	SG	70.40	134.91	29.19	9.52	4.47	2.58
1.00	SC	17.13	54.82	17.60	5.24	2.32	1.42
	SCC	16.90	34.13	9.15	4.26	2.25	1.42
	SE	43.95	154.87	110.60	99.32	95.63	94.18
	SG	34.40	80.44	13.14	4.49	2.21	1.41
1.25	SC	11.54	33.42	9.15	2.76	1.42	1.09
	SCC	11.35	21.41	6.11	2.59	1.42	1.08
	SE	24.90	111.81	72.85	64.84	61.87	60.84
	SG	18.53	47.45	7.19	2.57	1.41	1.09
1.50	SC	8.35	23.22	5.25	1.74	1.12	1.01
	SCC	8.25	15.23	4.29	1.73	1.12	1.01
	SE	14.94	80.84	49.37	43.31	41.19	39.95
	SG	11.18	29.29	4.48	1.72	1.12	1.01
1.75	SC	6.31	17.09	3.33	1.31	1.03	1.00
	SCC	6.24	11.54	3.05	1.31	1.03	1.00
	SE	9.44	59.28	34.20	29.60	27.84	27.00
	SG	7.39	19.06	3.05	1.31	1.03	1.00
2.00	SC	4.85	12.99	2.32	1.12	1.00	1.00
	SCC	4.81	9.17	2.25	1.12	1.00	1.00
	SE	6.30	43.88	24.12	20.59	19.28	18.81
	SG	5.21	13.10	2.22	1.12	1.00	1.00
2.25	SC	3.81	10.10	1.75	1.04	1.00	1.00
	SCC	3.77	7.43	1.73	1.04	1.00	1.00
	SE	4.43	32.77	17.47	14.80	13.75	13.34
	SG	3.85	9.54	1.71	1.04	1.00	1.00
2.50	SC	2.99	7.93	1.42	1.01	1.00	1.00
	SCC	2.98	6.13	1.42	1.01	1.00	1.00
	SE	3.24	24.97	12.83	10.86	10.10	9.72
	SG	2.96	7.21	1.41	1.01	1.00	1.00
2.75	SC	2.41	6.26	1.23	1.00	1.00	1.00
	SCC	2.40	5.10	1.23	1.00	1.00	1.00
	SE	2.48	19.14	9.69	8.07	7.52	7.31
	SG	2.37	5.60	1.23	1.00	1.00	1.00
3.00	SC	1.97	5.00	1.12	1.00	1.00	1.00
	SCC	1.97	4.27	1.12	1.00	1.00	1.00
	SE	2.00	14.93	7.38	6.18	5.75	5.62
	SG	1.94	4.49	1.12	1.00	1.00	1.00
3.50	SC	1.45	3.28	1.03	1.00	1.00	1.00
	SCC	1.45	3.05	1.03	1.00	1.00	1.00
	SE	1.45	9.51	4.65	3.90	3.64	3.53
	SG	1.44	3.04	1.03	1.00	1.00	1.00
4.00	SC	1.19	2.30	1.00	1.00	1.00	1.00
	SCC	1.19	2.25	1.00	1.00	1.00	1.00
	SE	1.19	6.33	3.13	2.66	2.51	2.45
	SG	1.18	2.22	1.00	1.00	1.00	1.00
5.00	SC	1.02	1.42	1.00	1.00	1.00	1.00
	SCC	1.02	1.42	1.00	1.00	1.00	1.00
	SE	1.02	3.24	1.78	1.57	1.50	1.47
	SG	1.02	1.42	1.00	1.00	1.00	1.00

Note: SC - Shewhart-CUSUM; SCC - Shewhart-CCUSUM; SE - Shewhart-EWMA; and SG - Shewhart-GWMA.

Table 7
RARL, EQL, and PCI performance comparison for the covariate model with different values of *B*.

Chart	*B*→	No Error	1	2	3	4	5
SC	RARL	3.75	1.53	1.20	0.71	0.57	0.51
	EQL	45.76	18.86	14.27	9.65	8.52	8.11
	PCI	3.25	1.34	1.01	0.68	0.60	0.58
SCC	RARL	1.52	2.87	0.89	0.59	0.50	0.47
	EQL	18.75	35.92	11.70	8.85	8.17	7.93
	PCI	1.33	2.55	0.83	0.63	0.58	0.56
SE	RARL	2.29	9.90	6.03	5.32	5.06	4.96
	EQL	26.21	127.89	74.00	64.54	61.16	59.71
	PCI	1.86	9.07	5.25	4.58	4.34	4.23
SG	RARL	2.01	4.08	1.10	0.67	0.55	0.50
	EQL	23.24	48.66	13.29	9.35	8.38	8.04
	PCI	1.65	3.45	0.94	0.66	0.59	0.57

Note: SC - Shewhart-CUSUM; SCC - Shewhart-CCUSUM; SE - Shewhart-EWMA; and SG - Shewhart-GWMA.

4.1. Effect of A and B on the performance of different combined control charts

Following the procedure shown by Maravelakis (2012), the ARL, RARL, EQL, and PCI values for the covariate model in Eq. (10) for different values B are presented in Tables 6-7. These ARL_1 profiles are computed with the same parameters of all the charts as in Table 5. We observe that as the value of B increases, the power of the combined charts to detect shift in the process mean increases. For instance, for the Shewhart-CUSUM chart, when B increases from 1 up to 3, the RARL, EQL, PCI decrease down to a large extent, from 3.75, 45.76, 3.25 to 0.71, 9.65, 0.68. When B increases from 3 up to 5, these measures decrease down to a small extent, from 0.71, 9.65, 0.68 to 0.51, 8.11, 0.58. Moreover, it has to state also that A does not affect the ARL performance of the combined charts in this study. This result is in accordance with Maravelakis (2012) and Linna & Woodall (2001).

5. A simulated example

In this section, we considered a simulated dataset to demonstrate the implementation of the combined charts with and without measurement errors when detecting a shift in the process mean.

Suppose that the underlying process $\{X_t\}$ is normally distributed for $t > 1$. We assume that this process remains in the IC state for $t \leq t_0$ with the process parameters $\{\mu = 0, \sigma = 1$ with $\gamma = 0.0\}$. A process in statistical control generates the first thirty observations, and the next twenty observations are generated from a process with an upward process shift ($t_0 = 30, 20$), respectively, with $\delta = 0.25$ when $t > t_0$. These data are then plotted in the two-sided combined charts. For the sake of concision, we only discuss the following three possible measurement error scenarios: no errors ($\gamma = 0$), error variation equal to 40% of the process variation ($\gamma = 0.4$), and equal to 90% error variation in the process ($\gamma = 0.9$), respectively.

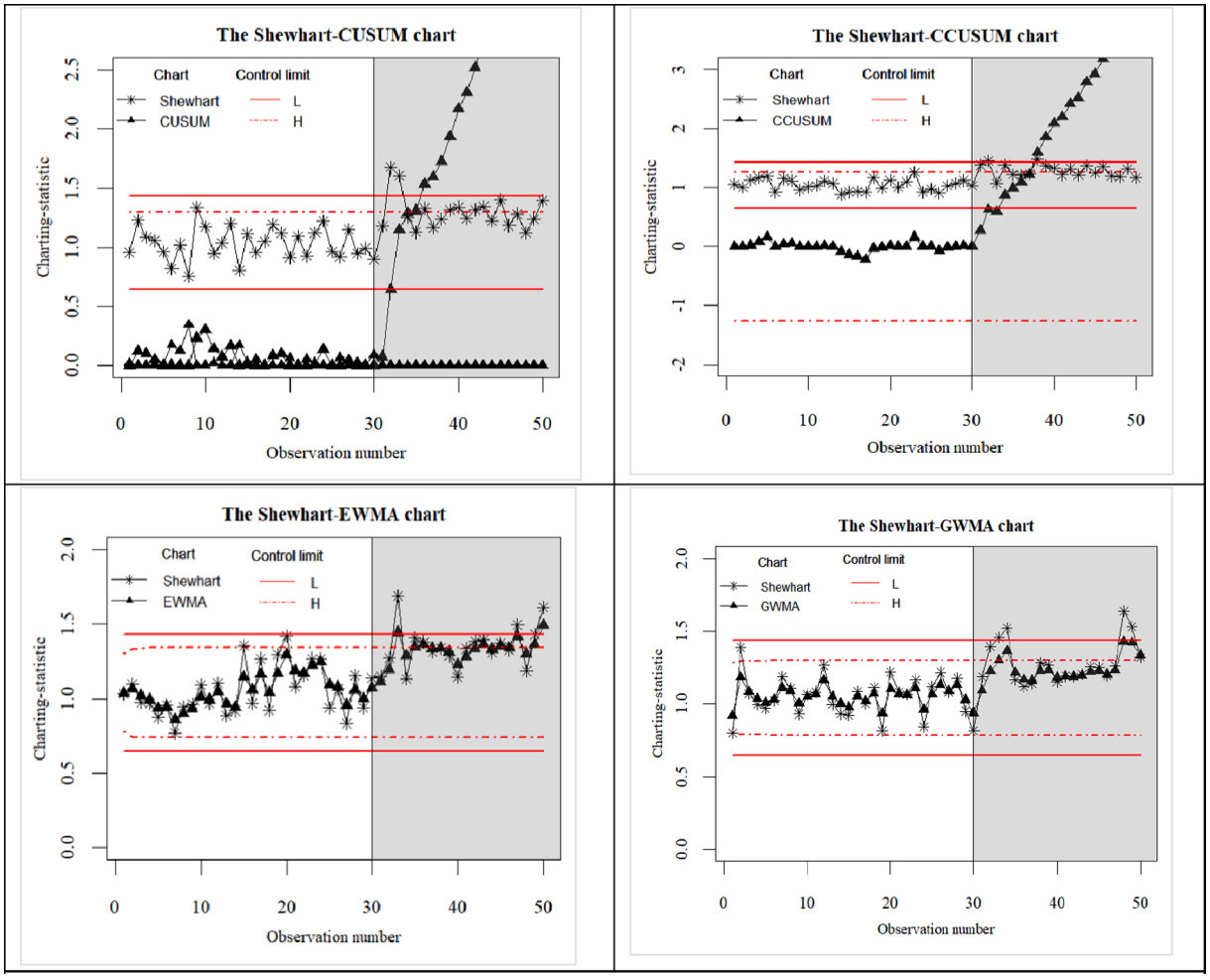

Fig. 5. The control charts applied to the simulated dataset at $\gamma = 0$.

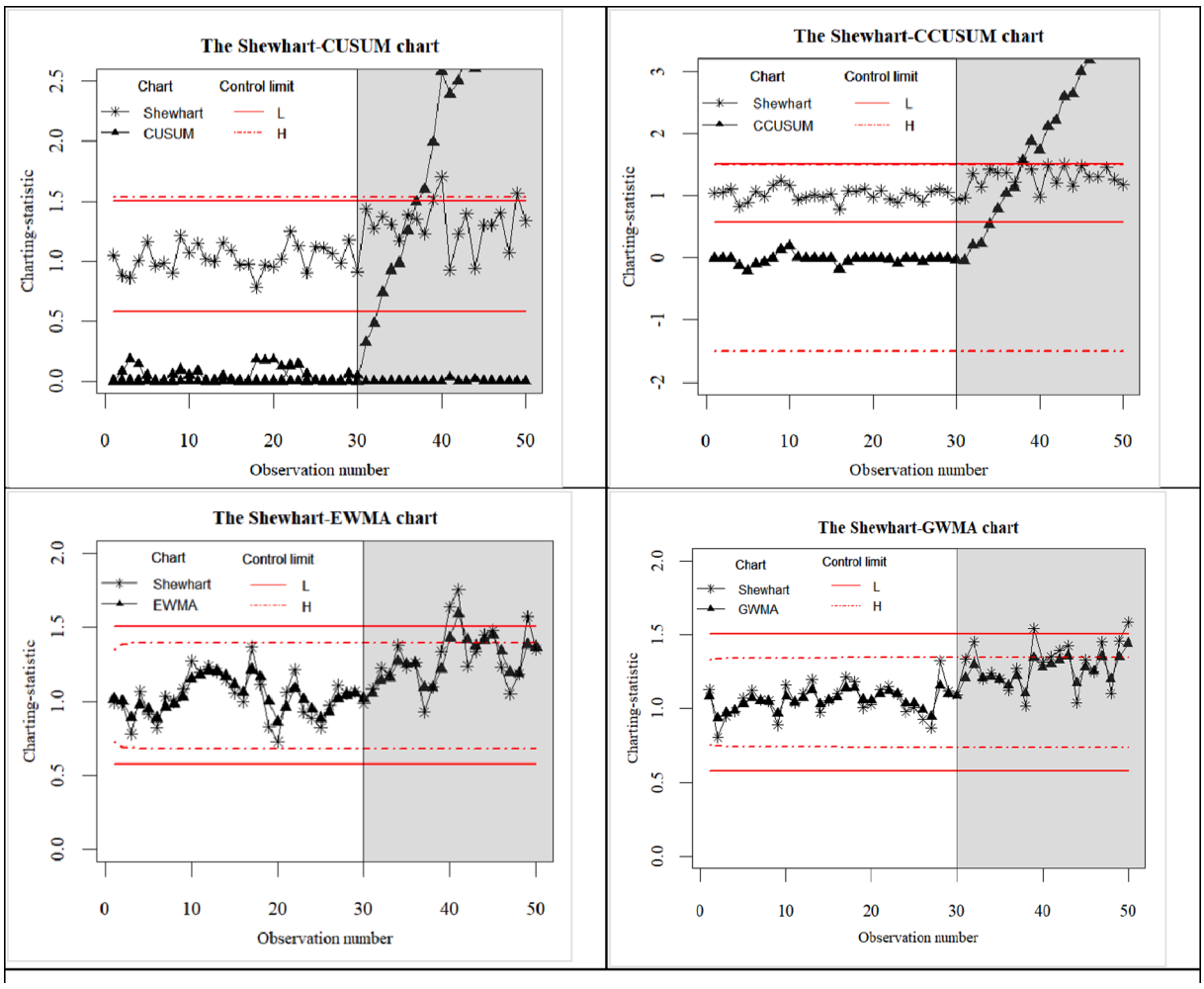

Fig. 6. The control charts applied to the simulated dataset at $\gamma = 0.4$.

The chart parameters for Shewhart-CUSUM, Shewhart-CCUSUM, Shewhart-EWMA and Shewhart-GWMA are: $(k = 0.5; h = 9.9; L_1 = 3)$, $(k = 0.5; h = 9.7; L_1 = 3)$, $(\lambda = 0.5; L_2 = 4; L_1 = 3)$ and $(\alpha = 0.5; q = 0.5; L_3 = 3.7; L_1 = 3)$, respectively. These parameters ensure an ARL of 370 of the corresponding charts for IC processes. Figs. 5-7 show the charts.

The above figures show how the statistical power of the charts deteriorates as measurement error increases. When there is no measurement error variation, the Shewhart-CUSUM, Shewhart-CCUSUM, Shewhart-EWMA and Shewhart-GWMA charts initiate the first OC signal at sample numbers (32, 32, 33, and 33). With $\gamma = 0.4$, the OC signals appear at (38, 38, 40, and 39), while with $\gamma = 0.9$ they appear at observations (43, 42, 46, and 46), respectively. These findings support the results of Section 5 that measurement error significantly impacts the performance of the combined charts.

6. Conclusion

In this study, we have investigated the performance of the well-established combined control charts for monitoring the normally distributed process mean parameter in the presence of measurement uncertainty, namely the Shewhart-CUSUM, Shewhart-CCUSUM, Shewhart-EWMA, and Shewhart-GWMA charts. A detailed run length profiles in terms of ARL, EQL, RARL and PCI, of these charts, have been computed using the Monte Carlo simulation method under different magnitudes of measurement errors. We found that while all charts were significantly impacted by measurement error, the Shewhart-CCUSUM had a better overall performance than the others, while Shewhart-EWMA performed the worst chart. We also note that taking multiple measurements per item in each sample can compensate for the negative effect of measurement inaccuracy. When measurement errors are inevitable, we recommend that practitioners use measurement uncertainty-based combined charts.

For future research, combined charts can be designed to combinedly deal with violating assumption of normality and perfect measurement data, on the lines of Rahlm (1985). This study can also be extended under the combined effect of measurement uncertainty and autocorrelation on the lines of Costa & Castagliola (2011). Additionally, the combined charts could be developed for profile monitoring in the presence of measurement errors, continuing the work by Noorossana & Zerehsaz (2015).

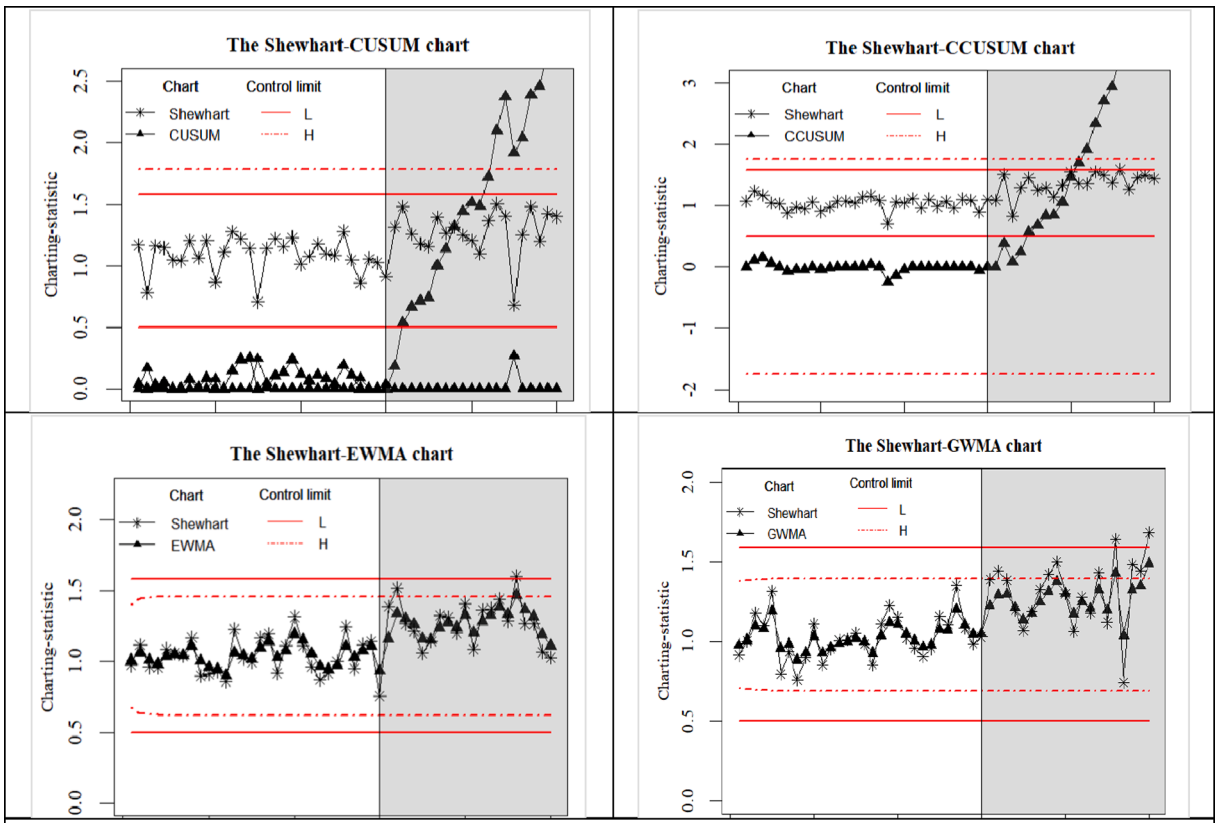

Fig. 7. The control charts applied to the simulated dataset at $\gamma = 0.9$.

CRediT authorship contribution statement

Tahir Munir: Conceptualization, Methodology, Software, Visualization, Formal analysis, Writing – original draft. **Xuelong Hu:** Conceptualization, Methodology, Software, Visualization, Formal analysis, Writing – original draft. **Osmo Kauppila:** Writing – review & editing, Investigation. **Bjarne Bergquist:** Writing – review & editing, Investigation.

Declaration of Competing Interest

The authors declare that they have no known competing financial interests or personal relationships that could have appeared to influence the work reported in this paper.

Data availability

Data will be made available on request.

Acknowledgments

The authors would like to thank all the reviewers for their detailed comments and helpful suggestions, which greatly helped in the improvement of the manuscript. This research was supported by these foundations: Foundation of Nanjing University of Posts and Telecommunications (No. NY222176), The Excellent Innovation Teams of Philosophy and Social Science in Jiangsu Province (No. 2017ZSTD022) and Key Research Base of Philosophy and Social Sciences in Jiangsu - Information Industry Integration Innovation and Emergency Management Research Center.

References

Abraham, B. (1977). Control charts and measurement error. *Annual Technical Conference of the American Society for Quality Control, 31*, 370–374.
Bennett, C. A. (1954). Effect of measurement error on chemical process control. *Industrial Quality Control, 10*, 17–20.
Costa, A. F., & Castagliola, P. (2011). Effect of measurement error and autocorrelation on the X chart. *Journal of Applied Statistics, 38*(4), 661–673.
Crosier, R. B. (1986). A new two-sided cumulative sum quality control scheme. *Technometrics, 28*(3), 187–194.
Hemmati, M. M., Amiri, A., & Jalilibal, Z. (2022). Designing a run sum control chart for monitoring multivariate coefficient of variation in the presence of measurement errors. *Sharif Journal of Industrial Engineering & Management., 38*(1), 111–117.
Kanazuka, T. (1986). The effect of measurement error on the power of X-R charts. *Journal of Quality Technology, 18*(2), 91–95.
Li, Q., Yang, J., Huang, S., & Zhao, Y. (2022). Generally weighted moving average control chart for monitoring two-parameter exponential distribution with measurement errors. *Computers & Industrial Engineering, 165*, Article 107902.
Linna, K. W., & Woodall, W. H. (2001). Effect of measurement error on Shewhart control charts. *Journal of Quality Technology, 33*(2), 213–222.
Lucas, J. M. (1982). Combined Shewhart-CUSUM quality control schemes. *Journal of Quality Technology, 14*(2), 51–59.
Lucas, J. M., & Saccucci, M. S. (1990). Exponentially weighted moving average control schemes: Properties and enhancements. *Technometrics, 32*(1), 1–12.
Maleki, M. R., Amiri, A., & Castagliola, P. (2017). Measurement errors in statistical process monitoring: A literature review. *Computers & Industrial Engineering, 103*, 316–329.
Maravelakis, P. E. (2012). Measurement error effect on the CUSUM control chart. *Journal of Applied Statistics, 39*(2), 323–336.
Montgomery, D. C. (2012). *Introduction to Statistical Quality Control* (7th Edition.). Wiley.
Nguyen, H. D., Tran, K. P., & Tran, K. D. (2021). The effect of measurement errors on the performance of the Exponentially Weighted Moving Average control charts for the Ratio of Two Normally Distributed Variables. *European Journal of Operational Research, 293*(1), 203–218.
Noorossana, R., & Zerehsaz, Y. (2015). Effect of measurement error on phase II monitoring of simple linear profiles. *The International Journal of Advanced Manufacturing Technology, 79*(9), 2031–2040.
Page, E. (1954). Continuous inspection schemes. *Biometrika, 41*(1/2), 100–115.
Park, C., Ouyang, L., & Wang, M. (2021). Robust g-type quality control charts for monitoring nonconformities. *Computers & Industrial Engineering, 162*, Article 107765.
Rahlm, M. A. (1985). Economic model of X-chart under non-normality and measurement errors. *Computers & Operations Research, 12*(3), 291–299.

International Organization for Standardization. (1994). Accuracy (trueness and precision) of measurement methods and results-Part 1: General principles and definitions (ISO 5725-1).

Rehman, A., Sabbir, J., Munir, T., Ahmad, S., Muhammad, R. (2022). New combined Shewhart-Memory-type mean charts. *Scientia Iranica*. (Revision submitted).

Riaz, M. (2014). Monitoring of process parameters under measurement errors. *Journal of Testing and Evaluation, 42*, 980–988.

Roberts, S. W. (1959). Control chart tests based on geometric moving averages. *Technometrics, 1*(3), 239–250.

Sheu, S. H., & Lin, T. C. (2003). The generally weighted moving average control chart for detecting small shifts in the process mean. *Quality Engineering, 16*(2), 209–231.

Thanwane, M., Malela-Majika, J. C., Castagliola, P., & Shongwe, S. C. (2021). The effect of measurement errors on the performance of the homogenously weighted moving average $\overline{X}$ monitoring scheme. *Transactions of the Institute of Measurement and Control, 43*(3), 728–745.

Umar, A. A., Khoo, M. B., Saha, S., & Haq, A. (2022). Effect of measurement errors on triple sampling X chart. *Quality and Reliability Engineering International, 38*(4), 1886–1908.

Yousefi, S., Maleki, M. R., Salmasnia, A., & Anbohi, M. K. (2022). Performance of Multivariate Homogeneously Weighted Moving Average Chart for Monitoring the Process Mean in the Presence of Measurement Errors. *Journal of Advanced Manufacturing Systems*, 1–14.